Fermilab

TM-1086
1183.000
July, 1982

Kermas for Various Substances Averaged Over the Energy Spectra of Fast Neutron Therapy Beams: A Study in Uncertainties.

M. Awschalom, I. Rosenberg, A. Mravca[(a)]
Fermi National Accelerator Laboratory
P. O. Box 500, Batavia, Illinois 60510

ABSTRACT

Kermas for various substances averaged over the energy spectra of fast neutron therapy beams, as well as ratios of average kermas relative to muscle, were calculated in an attempt to estimate the uncertainties introduced in these quantities by the poor knowledge of the elemental kerma functions, actual neutron energy spectra, and composition of tissues and other materials. Average kermas have uncertainties of the order of 7-25%, while for ratios of average kermas the uncertainties are of the order of 2-5% for materials of clinical interest.

It is concluded that the ratio of average kerma of muscle to A-150 T.E. plastic should be 0.93 $\pm$.03 for the new p+Be clinical neutron beams.

KEY WORDS: kermas, kerma ratios, neutron, neutron energy spectra, compositions, uncertainties

INTRODUCTION

Kerma functions,[1,2] expressed in terms of incident neutron energies for elements found in tissues and materials suitable for dosimetry, are useful to: (1) calculate the neutron energy deposited in tissue from knowledge of the energy spectrum and fluence; (2) calculate the dose that various tissues would have absorbed if the dose absorbed by a dosimeter is known; and (3) compare the energy deposited in various tissues by a given fluence having a known neutron energy spectrum.

In general, the ratios of the average kermas for tissues and dosimetry materials of interest to that of muscle are the quantities of greatest interest. These average kermas are calculated using the following averaging procedure:

$\bar{K}_m$ = average kerma for muscle, and

$\bar{K}_t$ = average kerma for material t

$$= \sum_j \alpha_j \bar{K}_j \; / \; \sum_j \alpha_j \qquad (1)$$

where:

j = chemical elements in material t,

α_j = mass fraction of j^{th} element in material t,

$\bar{K}_j$ = average kerma for jth element in the given neutron energy spectrum.

The quantities $\bar{K}_j$ are, in turn, obtained through the following averaging procedure:

$$\bar{K}_j = C \int_0^\infty K_j(E) N(E) dE \qquad (2)$$

where:

E = neutron energy,

$K_j(E)$ = kerma of the j^{th} element as a function of neutron energy,

$N(E)$ = neutron energy spectrum, and

C = normalizing factor, such that:

$$C^{-1} = \int_0^\infty N(E) dE. \qquad (3)$$

In this paper we investigate how the uncertainties in α_j, $K_j(E)$ and $N(E)$ affect estimates of K_t and their ratios to K_m for various therapeutic neutron beams. Bewley[3] had previously published similar work. However, since then more kerma function calculations have been made by various authors, the p+Be clinical neutron beams have become of more practical importance and their spectra are better understood.

ELEMENTAL COMPOSITIONS, α_j, AND THEIR UNCERTAINTIES

The elemental compositions assumed for various tissues and for materials suitable for fabrication of dosimeters are given in Tables I and II. The compositions of most tissues were taken from ICRP 23[4] or ICRU 26.[5] Other sources for elemental composition are Randolph,[6] Kim[7], White et al.[8], Constantinou[9] and references therein. Only the four major component elements, H, C, N and O are shown separately. Eight additional elements, however, were included in the computations: F, Na, Mg, P, S, Cl, K and Ca (and Ar for air). The sum of their mass fractions is also given in Tables I and II under "others". The sum total of all elemental mass fractions derived from the references is given in the column labelled $\sum\alpha_j$. Where this total was different from unity, the missing mass was added to the oxygen fraction for computational purposes.

The composition of human tissues has been studied with great detail with respect to trace elements, for environmental and biochemical reasons,[10] but scant attention has been paid to the relative abundance of the major components, H, C, N and O. Thus, the mass fractions quoted for most tissues in Table I are actually only quotients of two numbers with two significant digits given in ICRP 23.[4] The uncertainties in the relative abundances of the four main elements therefore lie between 1 and 9%. This state of

affairs is made worse by the large variation in average kerma that a small variation in hydrogen mass fraction will effect. In an attempt to estimate these uncertainties, compositions derived from different, and possibly independent, sources for muscle, bone and fat were used in the calculations.

Muscle Tissue. The reference composition adopted was that given in ICRU 26,[5] with the relative abundance of trace elements derived from ICRP 23.[4] The compositions given in ICRP 23[4] and by Yamamoto et al.[11] were also used in the calculations. (Table II).

Bone. The uncertainties in the composition of bone are complicated by the use of the generic term "bone" to denote different anatomical structures. Strictly speaking, these are not variations of the same material, and rather larger uncertainties than necessary would arise from considering them as such. Nonetheless, such a choice was adopted here because in most practical cases it would be very difficult to separate the various kinds of bone. Thus, besides the composition for compact femur given in ICRU 26,[5] other versions were used in the calculations: cortical bone from ICRP 23,[4] mouse metaphyseal bone from Epp et al,[12] which was considered close to human trabercular bone, human cortical bone from Woodard[13] and two versions of bone given by Kim[7] (Table II). The "inner bone" composition given by White et al.[8] was not used, as it is really a mixture of hard bone and red marrow.

Fat. Some of the above remarks also apply to the lumping of different adipose tissues under the blanket term "fat". For the same reason, though, different sources were used as variations to the reference subcutaneous adipose tissue given in ICRP 23:[4] fat from rat tissue from Yamamoto et al.[11] and human tristearin as given by Hawk et al.[14] (Table II).

A-150. The composition of dosimetry materials are somewhat better known than those of tissues, at least in principle. Variations in manufacture, however, can introduce some uncertainties. One of the most important materials for neutron dosimetry, A-150 tissue equivalent (T.E.) plastic, has received close scrutiny[15,16] and an estimate of the composition uncertainties can thus be formed. The recommended composition given by Smathers et al.[15] (Table II), with a quoted uncertainty of ±1%, is used as reference. The design goal and the average measured composition given by Goodman,[16] (Table II) are used as variations in the calculations.

Nylon. The danger in using generic names is illustrated in the case of Nylon.[17] Three different types of Nylon are actually listed in Appendix B of ICRU 26,[5] with substantially different compositions (Table II). All three versions were used in the calculations to estimate the uncertainties which would arise from careless use of presumably the same material.

ENERGY SPECTRA, N(E), AND THEIR UNCERTAINTIES

The fast neutron beams of interest in clinical applications are generally produced by either the exoergic d+D[18] or d+T[19,20] reactions using low energy high current beams or the high energy bombardment, at low currents, of thick or semi-thick beryllium targets by deuterons or protons.[21,22]

New neutron therapy facilities are planning the use of p+Be neutron beams while some of the old facilities using d+Be neutrons are planning a change to p+Be neutrons.[22] In view of this state of affairs, seven neutron energy spectra, grouped by method of production, were chosen for this study.

Those energy spectra which have been published by the various clinical facilities have two characteristics in common: the spectra have no uncertainties assigned to them and the low energy ranges of the spectra are missing. Therefore, low energy distributions were added to most spectra. These additions were varied in order to study their influence on the average kermas and kerma ratios. These and other changes are discussed below.

Protons on Beryllium. The general shape of these spectra was obtained, for energies above a few MeV, from published spectra for the p(35)Be,[23,24] p(41)Be[25] and p(46)Be[24] reactions.[(b)] These

results show a practically flat direct reaction distribution up to near the kinematic limit, and a fast rising low energy tail. This low energy contribution was approximated by an evaporation energy distribution. The final expression used for the reference spectra was:

$$N(E) = B(1 + A\sqrt{E}\, e^{-E/\Phi}) \qquad (4)$$

where Φ is an effective nuclear temperature (taken as 2.5 MeV), A is a scaling factor for the evaporation part of the spectrum, chosen to fit the experimental results,[24,25] and B is a normalizing factor that includes an appropriate cut-off at the kinematic limit. The resulting spectra for the selected p+Be beams are shown in Fig. 1 with solid lines.

1. p(66)Be. This beam was selected to represent the most penetrating beam now in use in the USA, p(66)Be(49) at Fermilab.[26,27] It also represents the p(60)Be(?) beam planned at Clatterbridge, England,[28] and the new p(65)Be(?) beam at Louvain-la-Neuve, Belgium.[29] The spectrum shown in Fig. 1 was estimated from lower energy p+Be measurements.[24,25] The earlier measurements of p+Be spectra at 35 and 65 MeV by Amols et al.[30] have effectively been retracted.[23]

2. p(41)Be. This beam is representative of the p(42)Be(15),

p(43)Be(20), p(46)Be(?) and p(48)Be(?) beams to be used at M. D. Anderson Hospital[31], the Cleveland Clinic,[32] UCLA Medical School[33] and University of Washington Medical School[28] in the USA, respectively. The 41 MeV proton energy was selected for easy comparison with experimental data.[25]

Four variations of the low energy spectral distributions are shown in Fig. 1. They were calculated for both spectra, but are only shown for the p(41)Be spectrum, for clarity. In two of these variations, (i) and (ii), the relative contribution of the evaporation neutrons was decreased or increased by halving or doubling the value of A in Eq. 4. In variation (iii), an E^{-1} spectrum was added and matched to the peak of the evaporation component. Variation (iv), representing a heavily filtered beam,[25] was obtained by eliminating the evaporation contribution altogether. In addition, for the p(41)Be beam, the measured unfiltered spectrum,[25] with an E^{-1} tail matched to its lowest measured energy point, was also used in the calculations as variation (v).

Deuterons on Beryllium. Measured spectra were used for these beams whenever possible. Three deuteron energies, in past or present clinical use, were selected.

3. d(49)Be. This beam was used for many years at M. D. Anderson

Hospital[34] before the acquisition of the p(42)Be(15) system. The reference spectrum was taken as that measured by Meulders et al.[35] for the d(50)Be reaction (curve D in Fig. 1, Ref. 25). This spectrum was extrapolated to near zero neutron energy using an exponential low energy distribution adapted from that measured by Greenwood et al.[36] at 40 MeV. Spectral variations were obtained by using: (i) the d(49)Be spectrum measured at TAMVEC (curve A in Fig. 1, Ref. 25), with an E^{-1} low energy distribution, matched to the lowest measured energy point, and (ii) the calculated heavily filtered spectrum (curve E in Fig. 1, Ref. 25), this time with a constant neutron flux extrapolation to near zero energy, matched to the lowest given energy point.

4. d(22)Be. This beam represents the d(21.5)Be(16) beam that has been extensively used at the Medical School of the University of Washington, Seattle.[34] It is also representative of the d(25)Be beam previously used at the Cleveland Clinic.[37] As the energy spectrum of this beam has not been measured, the average obtained by combining the d(20)Be and d(24)Be spectra, as given in Ref. 21, page 14, was used. No spectral variations were calculated for this beam.

5. d(16)Be. This is one of the oldest clinical neutron beams, albeit of low penetration. It was used in the pioneering work of Catterall and Bewley in reviving interest in fast neutron therapy.[21,38] A similar d(15)Be beam is also currently in use in

Edinburgh, Scotland,[39] and a d(14)Be beam is being used for therapy in Essen, West Germany.[40] The reference spectrum used was taken from Ref. 24, with an exponential extrapolation to near zero neutron energy, adopted from Greenwood et al.,[36] matched to the lowest measured energy point. Two variations were used: (i) the above spectrum with an E^{-1} low energy distribution and (ii) the spectrum given in Ref. 21, page 14, with a linear extrapolation to the origin. These choices span the range of spectral shapes recently derived for various field sizes and depths in phantom.[41] The three versions of the d(16)Be spectrum are shown in Fig. 2, where they are arbitrarily matched at the peak.

Exoergic Reactions

6. d+T. This is a popular clinical neutron beam in Europe.[22] It starts as a nearly monochromatic beam (14.7 MeV),[19] but degrades into a continuous energy spectrum beam as it traverses tissues.[40,42,43] The 14.7 MeV monochromatic beam was taken as the reference. The degraded spectra at 2 cm, 7 cm and 17 cm deep in tissue[42] were also used as variations in the calculations.

7. d(8.3)D. This is another one of the low penetration beams.[18,44] It might be the forerunner of the "poor person" clinical neutron beam. The calculated energy spectrum was used.[18] No variations of this spectrum were considered.

KERMA FUNCTIONS $K_j(E)$ AND THEIR UNCERTAINTIES

There are numerous available calculations of elemental kerma functions.[45-59] Their very existence indicates the uncertain knowledge of the energy deposition processes, especially at energies higher than about 15 MeV. Some of the more recent calculations were used to obtain a reference set of kerma functions.

Hydrogen. Two sets of calculations exist in the 0 to 30 MeV energy range, Caswell et al.[45] and Fleming[46]. At higher neutron energies calculations have been published by Alsmiller et al.[48] (20 to 70 MeV), Behrooz et al.,[49,50] (14 to 60 MeV), Bassel et al.[47] (30 to 100 MeV), and Wells[58] (10 to 80 MeV) (Figure 3). For the reference set, the values calculated by Caswell et al.[45] and Behrooz et al. [50] were adopted because they represent the most recent calculations.

Carbon, Nitrogen and Oxygen. The most recent calculations in the 0 to 30 MeV energy range are those of Caswell et al.[45] At higher neutron energies calculations have been published by Alsmiller et al.[48] (20 to 70 MeV), Behrooz et al.[49,50] (14 to 60 MeV), Brenner et al.[51-53] (10 to 80 MeV), Dimbylow[54-57] (10 to 60 MeV), Wells[58] (10 to 80 MeV), and Herling et al.[59] (27 to 61 MeV). A reference kerma set for neutron energies greater than 10 to 20 MeV was

chosen from the latest published calculations of the groups listed above.[48,50,53,56,58]. (Figs. 4-6) The work of Herling et al.[59] was not included because the number of neutron energies for which kerma value calculations are given are too few to allow meaningful interpolations.

The kerma values for these elements calculated by each group at 27.4, 39.7, and 60.7 MeV were compared with the values measured by Brady et al.[60] (Table III) using a weighted deviation algorithm of the form $\sum k_e|1-(k_e/k_c)|$, where k_e and k_c are the experimental and calculated kerma values, respectively, for each element. The summation was over the three energies listed above. The kerma sets with the lowest value for this algorithm were: for carbon, Dimbylow[56]; for nitrogen, Behrooz et al.[50]; and for oxygen, Wells[58] (Table III). These kerma functions were, therefore, selected to form the reference set, since they agree most closely with the measured values. However, the experimental values themselves have large uncertainties[60] and it is not certain that the selected set of kerma values is the best one. More measurements of kermas are indeed needed.

Change-Over Energy. There is an overlap between the calculated kerma functions of Caswell et al.[45] and the higher energy calculations. However, the former become less reliable above 10 MeV and especially above 15 MeV,[61] while reservations have been expressed about the reliability of some higher energy calculations

below about 14 MeV,[52] and other calculated functions do not have values below this energy.[48,50] Therefore, a change-over was effected from the calculations of Caswell et al.[45] to the selected higher energy kerma functions, at 15 MeV for the reference set and at various energies for the other kerma function combinations studied. These change-over energies are labelled in EX in Table IV.

Kerma Functions Combinations. In order to estimate the uncertainties in the calculated average kermas and kerma ratios due to the spread in the values of the above kerma functions, several combinations of these functions were used in the calculations (Table IV). The first combination shown in that table is the reference set of kerma functions, discussed above. The next five (II-VI) represent the most recent calculations of the authors mentioned above. Combinations VII and VIII were used to investigate how the choice of change-over energy from the Caswell et al.[45] kerma functions influenced the average kermas calculated using the reference set. In combinations IX to XVI, kerma functions which represent the extremes of the values shown in Figs 3-6 (in the range from 20 to 50 MeV) were combined, in turn, with the rest of the reference set.

Elements With Z>8. There are only two extensive sets of kerma calculations for these elements, Caswell et al.[45] below 30 MeV and Dimbylow[56] from 10 to 60 MeV. These functions were, therefore,

used with all the above kerma functions combinations with transitions at the appropriate change-over energies (Table IV). The kerma functions for the elements not calculated by Dimbylow[56] (F, Na, Cl and K) were assumed to be proportional to the functions of their nearest neighbors in the periodic table, the constant of proportionality being chosen to match the Caswell et al.[45] values at the change-over energy. As these elements constitute much less than 1% of most tissues and materials studied in this work (with the exception of A-150 plastic), the uncertainties introduced by the lack of knowledge of their kerma functions should be correspondingly small.

RESULTS AND DISCUSSION

The various energy spectra, kerma functions, and elemental compositions of tissues and materials were stored in a Cyber 175 computer[62] either in tabular form or as algorithms. Integration steps and limits were adjustable. It was possible to select any set of kerma functions over any energy range. The results of the calculations were displayed both as average kermas, $\overline{K}_t$, and ratios of average kermas relative to muscle $\overline{K}_t/\overline{K}_m$ (in short, kerma ratios or k_t), together with the partial kerma contribution for each element.

UNCERTAINTIES ARISING FROM VARIATIONS IN ELEMENTAL COMPOSITIONS.

The reference set of kerma functions (combination I in Table IV) was convoluted with the reference spectra for each of the seven therapy beams under study and with the various elemental compositions for muscle, bone, fat, A-150 plastic and Nylon given in Table II, to produce average kermas.

These average kermas, presented as ratios to ICRU Muscle ($\overline{K}_m$=100) are shown in Table V for all variations in composition of these five materials. The spread in kerma ratios is seen to be about 1.5% for muscle and about 1% for A-150. The spread in kerma ratios for bone, fat and Nylon is much larger, as expected from the discussion on tissue compositions. Even though its average kermas lie on one extreme of the range of muscle kerma values, the ICRU[5] version of muscle tissue was taken as reference, as this composition has been used extensively by many authors. The ICRP[4] versions of bone and fat composition, however, were chosen as references, as their kermas lie toward the middle of their respective kerma ranges. For both the above reasons, the composition of A-150 plastic recommended by Smathers et al.[15] was chosen as reference. Nylon type Zytel 69 was taken as the reference for this material, as its kerma also lies in the middle of the kerma range.

A summary of the variations in the kerma ratios shown in Table V is given in Table VI. Two methods to indicate these variations have been employed. The extreme differences from the reference values have been shown as $+\Delta_+$ and $-\Delta_-$ in the left hand side of each matrix box, while on the right hand side is shown a quantity $\pm \sigma_\alpha$, where:

$$\sigma_\alpha^2 = \frac{1}{N}\sum_i (k_i - k_{ref})^2 \qquad (5)$$

where k_{ref} and k_i represent entries in Table V for the reference composition and for each variation, respectively. Thus, σ_α is a kind of root mean square deviation from the reference kerma ratio, the subscript α denoting that the deviations were due to uncertainties in composition. The values of σ_α are seen to be remarkably similar for all energy spectra, at about 1.5% for muscle, 13% for bone, 4.5% for fat, 0.7% for A-150 and 3.5% for Nylon.

UNCERTAINTIES ARISING FROM VARIATIONS IN NEUTRON ENERGY SPECTRA

The reference set of kerma functions was convoluted with the elemental compositions of representative substances, as given in Tables I and II, and with the reference neutron energy spectra for the selected neutron therapy beams, as well as with all the spectral variations described in the appropriate preceding section. The resulting sets of average kermas are shown in Table

VII. In this Table, the kermas for muscle are given in units of 10^{-15} J kg^{-1} m^2n^{-1}, while the values for all other substances are kerma ratios relative to the corresponding average muscle kerma, (K_m = 100). The d(22)Be and d(8.3)D beams are not shown in this Table since no spectral variations were calculated for them.

A summary of the variations in kermas and kerma ratios shown in Table VII is given in Table VIII. As in the previous section, both the extreme differences $+\Delta_+$ and $-\Delta_-$ and an r.m.s. deviation $\pm\sigma_N$, estimated using Eq. 5, are shown in each matrix box.

In the case of the d+T beam a different approach was taken. As can be seen in Table VII, the monochromatic spectrum, taken as reference, and the three in-depth spectra produce two distinct sets of average kermas and kerma ratios. These variations are not, strictly speaking, a consequence of uncertainties in the spectrum, but of a known degradation of the neutron flux when scattered by tissue. Assigning a single average kerma to this beam for all depths, however, would introduce an error in dosimetry, especially if the value appropriate to the monochromatic spectrum is used. To obtain an estimate of this error, the means and standard deviations of the three in-depth average kermas and kerma ratios were first evaluated. The upper figures in Table VIII were obtained as the differences between the monochromatic K_m and k_t and these means, while the lower figures are the above mentioned standard deviations. The former set of

differences were then taken as σ_N for the d+T beam.

It can be seen from Table VIII that the uncertainties in the average kermas for muscle, K_m, introduced by the adopted variations in neutron energy spectra are quite large, ranging from 5% to 24%, and, in fact, dominate the total uncertainties for K_m. On the other hand, the deviations in kerma ratios for the p+Be and d+Be beams are, in general, well under 1%, even though rather extreme variations of the low energy end of these spectra were used to obtain them. The results of these calculations thus show that the inability to measure neutron energy spectra at low energies does not significantly influence the ratio of the average kermas.

UNCERTAINTIES ARISING FROM VARIATIONS IN KERMA FUNCTIONS

The reference elemental compositions of representative substances and the reference spectra for the seven selected clinical neutron beams were convoluted in turn with each kerma function combination given in Table IV. The resulting sets of average kermas and kerma ratios are given in Tables IX (a)-(d). There, again, the average kermas for muscle are given in units of 10^{-15} J kg^{-1} m^2 n^{-1}, while the values for all other substances are kerma ratios relative to the corresponding muscle average kerma ($\overline{K}_m$=100). It can be seen that, in general, the variations from the

reference kerma values produced by substituting one extreme elemental kerma function at a time (combinations IX to XVI) are much smaller than variations among different authors. Therefore, only combinations II to VIII were used to derive the r.m.s. deviations (Table X). In Table IX (d), only those kerma function combinations are shown that actually have different kerma functions over the energy ranges of the lower energy beams. For the d(16)Be, d+T and d(8.3)D beams, for example, where there is no neutron fluence above 15 MeV, only those combinations having cross-over energies below 15 MeV will introduce different kerma functions.

A summary of the variations in K_m and kerma ratios shown in Tables IX (a)-(d) is given in Table X. Again, both the extreme differences, $+\Delta_+$ and $-\Delta_-$, and estimated r.m.s. deviation, $\pm\sigma_K$, are shown in each matrix box. It can be seen from Table X that in most cases the deviations in average kermas and kerma ratios become progressively smaller for beams of decreasing mean neutron energy, with the exception of the monochromatic d+T beam. This trend is a reflection of the fact that the same kerma functions[45] were used below 10-20 MeV for all kerma combinations.

ADDITION OF UNCERTAINTIES

The ultimate goal of the calculations presented in this work is to estimate the total uncertainties in average kermas and kerma ratios arising from uncertainties in elemental composition, neutron energy spectra and elemental kerma functions.

The total uncertainties, σ, were calculated by adding in quadrature the individual uncertainties discussed above:

$$\sigma^2 = \sigma_\alpha^2 + \sigma_K^2 + \sigma_N^2 + \sigma_{\alpha M}^2 \qquad (6)$$

where the subscripts α, K and N refer to uncertainties arising from variations in elemental compositions, kerma functions and neutron energy spectra, respectively, and the last term, $\sigma_{\alpha M}^2$, is added only for kerma ratios and represents the contribution to the total uncertainty due to the fact that the reference material, muscle, has its own uncertainty in composition.

A summary of the results of the computations outlined in this paper is presented in Table XI. For each substance listed in this Table the following quantities are given: the average kerma (for muscle only) or kerma ratio relative to muscle ($\overline{K}_m = 100$) obtained by convoluting the reference composition, from Tables I or II, with the reference version of each of the seven selected spectra,

and with the reference set of kerma functions; the total uncertainty in this average kerma or kerma ratio, calculated using Eq. 6; and, in brackets, the percentage of the total average kerma contributed by the hydrogen atoms.

It is evident from the magnitude of the uncertainties associated with muscle average kermas derived in this work that only two significant digits would be warranted when displaying K_m in Table XI. These uncertainties would have been even larger if the overall uncertainties in the elemental kerma measurements, arising from normalization, numerical integration and statistics,[60] and the partial success of the calculations trying to reproduce them (Table III) had been taken into account. Therefore, the third digits in the display of $\overline{K}_m$ in Table XI have been enclosed in brackets, lest too much importance is attached to them. On the other hand, the uncertainties in kerma ratios were found to be consistently less than the corresponding uncertainties for $\overline{K}_m$, except where large composition variations were considered. Moreover, these uncertainties in kerma ratios should not be affected significantly by the above uncertainties in experimental values. The magnitudes of these uncertainties therefore may warrant the use of three significant digits when displaying reference values of kerma ratios in Table XI. In the previous tables, four digits were carried to minimize rounding errors and to display the sometime small variations in kerma ratios that were produced by large variations in assumptions.

The following criteria were used to estimate the total uncertainties σ.

(a) For those substances for which all three partial uncertainties σ_α, σ_N and σ_K were calculated, the calculation of σ was straightforward. As σ_N for the d(22)Be and d(8.3)D beams were not calculated, they were taken in all cases as the means of the values derived for the d(50)Be and d(16)Be beams.

(b) For those compounds for which σ_N and σ_K were calculated, but not σ_α (i. e. polyethylene and polystyrene), the values of σ_α for A-150 plastic were used in Eq. 6, as the uncertainties in manufacture are presumably similar.

(c) For water, graphite and air, for which only the σ_K and σ_N were calculated, the σ_α were set equal to zero. For the sake of conciseness, only water kerma variations were shown explicitly in the previous tables.

(d) For all tissues for which no uncertainties were calculated, the σ_α were assumed equal to the corresponding ones for muscle, $\sigma_{\alpha M}$. For most of them, except brain and yellow marrow, the composition is close to that of muscle; thus the σ_K and σ_N for water were used in Eq. 6, as variations in kerma functions and spectral distributions would affect the results to a similar extent.

(e) For brain and yellow marrow, which have compositions closer to fat than to muscle, the σ_K and σ_N for fat were used in Eq. 6.

(f) For other materials in Table XI (Lucite, Mylar and T.E. gas[63]), total uncertainties σ were assigned equal to the corresponding ones for A-150 plastic.

(g) In the case of T.E. solution,[64] no variations in neutron spectral energy distributions or kerma functions can affect its kerma ratios, because its composition is so close to that of reference muscle. Thus, zero values for σ_K and σ_N were used in Eq. 6, while values of σ_α equal to those for A-150 plastic were assumed,because of similar uncertainties in manufacture.

The kerma ratios for most substances listed in Table XI vary slowly across the range of neutron beam energies studied in this work. This tends to support the conclusions of Bewley[3] and Bonnett et al.[41] that kerma ratios change slowly with spectral degradation at depth in tissue, except for the initially monochromatic d+T beam (Table VII).

The present calculations show, moreover, that with the well-known exceptions of bone and fatty tissues, no significant differences in average kermas exist for most tissues and organs in the human body.

The values of kerma ratios shown in Table XI compare well with the calculations of Bewley,[3] who considered many of the same substances. This is true even for the p(66)Be beam, in spite of the use of quite different neutron energy spectra. There is disagreement, however, between the present estimates of kerma ratio uncertainties and Bewley's. Whereas uncertainties for tissues are larger in the present work, which includes uncertainties in elemental composition, the large uncertainty in the kerma ratio of A-150 T.E. plastic for the p(66)Be beam quoted by Bewley cannot be reconciled with our calculations (Table XII).

Estimates of the uncertainty in the kerma ratio of A-150 plastic to muscle are especially important in discussions concerning total uncertainties in neutron dosimetry using A-150 ionization chambers. The American Protocol for Neutron Beam Dosimetry[65] quotes a 2% value for this kerma ratio uncertainty for all beams, while the European Protocol quotes 2.6% to 9.7%, the latter figure applying to a p(66)Be beam.[66] From the present calculations, it would seem that a range of 2% to 5% in this uncertainty would be more appropriate. Within the above uncertainties, there is good agreement between the kerma ratios of A-150 to muscle presented in this work and those recommended by the other sources summarized in Table XII.

CONCLUSIONS.

A review of the unsatisfactory knowledge of elemental compositions of tissues and some materials, of the lack of information about the low energy range of clinical neutron beam energy spectra and of the spread in values among available kerma function calculations has led to estimates of total uncertainties in average kermas and kerma ratios relative to muscle. Average kermas for muscle have been estimated to have uncertainties of the order of 7-25%. Kerma ratios for materials of clinical interest, on the other hand, have uncertainties of the order of 2-5%.

The ratio of the average kerma of muscle relative to A-150 plastic, a quantity of central importance in neutron therapy dosimetry, should be taken as 0.93 $\pm$0.03 for the new p+Be clinical neutron beams.

ACKNOWLEDGMENTS

We are very much in debt to D. J. Brenner, J. F. Dicello, R. E. Prael, and M. Zaider of Los Alamos National Laboratory and Dr. P. J. Dimbylow of the N.R.P.B., Didcot, England who made available to us results of their elemental kerma function calculations before publication. We are grateful to Ms. Michelle Gleason who displayed unbelievable patience while typing this manuscript.

Last but not least, we thank that unknown referee who kept the first draft of this paper for about half a year thus allowing us to include references 53 and 56.

This investigation was supported by PHS Grant Number 5P01CA18081-07, awarded by the National Cancer Institute, DHHS.

REFERENCES

(a) Participant in Summer of 1979. Now at Hewlett-Packard Co., Brisbane, California.

(b) The expression p(66)Be(49) means that 66 MeV protons are incident on a semi-thick target. In this target, protons not undergoing nuclear scattering lose 49 MeV by ionization. p(66)Be would mean a thick target. p(66)Be(?) would mean that the target thickness is unknown.

1. ICRU Report No. 13, Neutron Fluence, Neutron Spectra and Kerma, International Commission on Radiation Units and Measurements, Washington, D. C., 1969.

2. ICRU Report No. 33, Radiation Quantities and Units, International Commission on Radiation Units and Measurements, Washington, D. C., 1980.

3. Bewley, D. K., Practical Kerma Values for Therapy Applications, Monograph on Ion chambers for Neutron Dosimetry, EUR 6782, Ed. by J. J. Broerse (Commission of the European Communities, Luxemburg), 1980.

4. ICRP Report No. 23, Report of the Task Group on Reference Man, International Commission for Radiological Protection, New York: Pergamon Press, 1975.

5. ICRU, Report No. 26, Neutron Dosimetry for Biology and Medicine, International Commission on Radiation Units and Measurements, Washington, D.C., 1977.

6. Randolph, H. L., "Measurements and Properties of Ionizing Radiations", Ch. I of "Physical Techniques in Biological Research", Vol. II, Part 8, 2nd Edition, Moore, D. D., Editor, Academic Press, New York, 1969.

7. Kim, Y. S., Human tissues: Chemical Composition and Photon Dosimetry Data, Radiation Research 57, 38 (1974).

8. White, D. R., Martin, R. J., and Darlison, R., Epoxy Resin Based Tissue Substitutes, Brit. J. of Radiol. 50, 814 (1977).

9. Constantinou, C., Phantom Materials for Radiation Dosimetry. I. Liquids and Gels, Brit. J. of Radiol. 55, 217 (1982).

10. Iyengard, G. V., Kollmer, W. E., Bowen, H. J. M., "The Elemental Composition of Human Tissues and Body Fluids". Weinheim: Verlag Chemie, New York, 1978.

11. Yamamoto, O., Sawada, S., Yoshinaga, H. Nippon Igakku Hoshasen Gakkai Zasshi (Nippon Acta Radiol.) 23, 141 (1963).

12. Epp, E. R., Woodard, H. Q., Weiss, H., Energy Absorption by the Bone Marrow of the Mouse Receiving Whole Body Irradiation with 250 keV X-rays or ^{60}Co Gamma Rays, Radiation Research 11, 184 (1959).

13. Woodard, H. Q., The Elementary Composition of Human Cortical Bone, Health Phys. 8, 513 (1962).

14. Hawk, P. B., Oser, B. L., Summerson, W. H., "Practical Physiological Chemistry", 13th Edition. McGraw Hill (Blakiston), New York. 1954.

15. J. B. Smathers, V. A. Otte, A. R. Smith, P. R. Almond, F. H. Attix, J. J. Spokas, W. M. Quam, L. J. Goodman, Composition of A-150 Tissue Equivalent Plastic, Med. Phys. 4, 74-77(1977).

16. Goodman, L. J., Density and Composition Uniformity of A-150 Tissue Equivalent Plastic, Phys. Med. Biol. 23, 753 (1978).

17. Trade name of E. I. DuPont de Nemours & Co.

18. Waterman, F. M., Kuchnir, F. T., Skaggs, L. S., Hendry, G. O., Tom, J. L., Dosimetric Properties of Neutron Beams from the D-D Reaction in the Energy Range from 6.8 to 11.1 MeV, Phys. Med. Biol. 23, 397 (1978).

19. Marion, J. B., Fowler, J. L., Fast Neutron Physics, New York: Interscience, 1960. 2 Vols. Chapter I.

20. Hilton, J. L., Hendry, G. O., On Achieving A Clinically Useful D-T Neutron Isocentric Therapy System, IEEE Trans. Nucl. Sci. NS-28, 1889 (1981).

21. Catterall, M., Bewley, D. K., Fast Neutrons in the Treatment of Cancer, London: Academic Press, 1979.

22. Cohen, L., Awschalom, M., Fast Neutron Radiation Therapy, Ann. Rev. Biophys. Bioeng., 11, 359 (1982).

23. Ullman, J. L., Peek, N., Johnsen, S. W., Raventos, A., Heintz, P., Improved Measurement of Neutron Spectrum from 35 MeV Protons on Thick Beryllium. Med. Phys. 8, 396 (1981).

24. Waterman, F. M., Kuchnir, F. t., Skaggs, L. S., Kouzes, R. T., Moore, W. H., Neutron Spectra from 35 and 46 MeV Protons, 16 and 28 MeV Deuterons, and 44 MeV ^{3}He Ions on Thick Beryllium, Med. Phys. 6, 432 (1979).

25. Graves, R. G., Smathers, J. B., Almond, P. R., Grant, W. H., Otte, V. A., Neutron Energy Spectra of d(49)Be and p(41)Be Neutron Radiotherapy Sources, Med. Phys. 6, 123 (1979).

26. Cohen, L., Awschalom, M., The Cancer Therapy Facility at the Fermi National Accelerator Laboratory, Batavia, Illinois. A Preliminary Report, Applied Radiology, 5, 51(1976).

27. Rosenberg, I., Awschalom, M., Characterization of a p(66)Be(49) Neutron Therapy Beam I: Central Axis Depth Dose and Off-Axis Ratios, Med. Phys. 8, 99 (1981).

28.Eenmaa, J., University of Washington Medical School, Seattle, Private Communication.

29. Vynckier, S., Pihet, P., Octave-Prignot, M., Meulders, J. P., and Wambersie, A., Comparison of Neutron Beams Produced by 50 MeV Deuterons and 65 MeV Protons for Radiotherapy, submitted for publication.

30. Amols, H. I., Dicello, J. F., Awschalom, M., Coulson, L., Johnsen, S. W., Theus, R. B., Physical Characterization of Neutron Beams Produced by Protons and Deuterons of Various Energies Bombarding Beryllium and Lithium Targets of Several Thicknesses, Med. Phys. 4, 486 (1977).

31. Otte, V., M. D. Anderson Hospital and Tumor Institute, Private Communication.

32. John Horton, The Cleveland Clinic, Cleveland, Ohio. Private Communication.

33. McDonald, J., UCLA Medical School. Private Communication.

34. Smith, A. R., Almond, P. R., Smathers, J. B., Otte, V. A., Attix, F. H., Theus, R. B., Wooton, P. Bichsel, H., Eenmaa, J. Williams, D., Bewley, D. K., Parnell, C. J., Dosimetry Intercomparisons Between Fast Neutron Radiotherapy Facilities, Med. Phys. 2, 195 (1975).

35. Meulders, J. P., Leleux, P., Macq, P. C., Pirart, C. Fast Neutron Yields and spectra from Targets of Varying Atomic Number Bombarded with Deuterons from 16 to 50 MeV, Phys. Med. Biol. 20, 235 (1975).

36. Greenwood, L. R., and Heinrich, R. R., Integral Tests of Neutron Activation cross Sections in a $^{9}Be(d,n)$ Field at E = 40 MeV, Nuclear Science and Engineering 72, 175 (1979).

37. Turco, R. F., Gehbauer, R., Rodriguez-Antunez, A., Horton, J. L., Roberts, W. K., and Blue, J. W., Status Report of the Cleveland Clinic Foundation National Aeronautics and Space Administration Neutron Therapy Center, page 150 in "Treatment Planning for External Beam Therapy with Neutrons", Ed. Burger, G., Urban & Schwarzenberg, Munchen, Wein, Baltimore, 1981.

38. Parnell, C. J., A Fast Neutron Spectrometer and Its Use in Determining the Energy Spectra of Some Cyclotron-Produced Fast Neutron Beams, British J. Radiol. 45, 452(1972).

39. Duncan, W., Williams, J. R., Redpath, A. T., and Arnott, S. J., Neutron Therapy Planning: Principles and Practice in Edinburgh, page 156 in "Treatment Planning for External Beam Therapy with Neutrons", Ed. Burger, G., Urban & Schwarzenberg, Munchen, Wein, Baltimore, 1981.

40. Schmidt, R., and Hess, A., Spectroscopic Intercomparison at the German Neutron Therapy Centers, Int. J. Radiat. Oncol. Biol. Phys. 8, 1511 (1982).

41. Bonnett, D. E., and Parnell, C. J., Effect of Variation in the Energy Spectrum of a Cyclotron Produced Fast Neutron Beam in a Phantom Relevant to Its Application in Radiotherapy, Brit. J. of Radiol. 55, 48 (1982).

42. Hannan, W. J., Porter, D., Lawson, R. C., Railton, R., Spectrum Measurements in 15 MeV Neutron Therapy Beams, Phys. Med. Biol. 18, 808 (1973).

43. Kudo, K., Energy Spectrum and Absorbed Dose in Water for d+T Neutron Irradiation, Phys. Med. Biol. 27, 905 (1982).

44. Kuchnir, F. T., Billings Hospital, University of Chicago, Private Communication.

45. Caswell, R. S., Coyne, J. J., Randoh, M. L., Kerma Factors for Neutron Energies Below 30 MeV, Radiat. Res. 83, 217 (1980).

46. Fleming, R. F., Energy Transfer to Hydrogen by Neutrons up to 30 MeV, Radiat. Research 60, 347 (1974).

47. Bassel, R. H., Herling, G. H., Energy Transfer to Hydrogen by Neutrons from 30 to 100 MeV, Radiat. Res. 69, 210 (1977).

48. Alsmiller, R. G., Barish, J., Neutron Kerma Factors for H, C, N, O and Tissue in the Energy Range of 20-70 MeV, Health Physics 33, 98 (1977).

49. Behrooz, M. A., Gillespie, E. J., Watt, D. E., Kerma Factors for Neutrons with Energies up to 60 MeV, Phys. Med. Biol. 26, 507(1981).

50. Behrooz, M. A., Watt, D. E., Kerma Factors for Neutrons of 14 MeV to 60 MeV in Elemental H, C, N, and O. Radiation Protection and Dosimetry 1, 291 (1981).

51. Brenner, D. J., Prael, R. E., Dicello, J. F., Zaider, M., Improved Calculations of Energy Deposition from Fast Neutrons, Proc. 4th Symp. Neutron Dosimetry in Biology and Medicine, Munich June 1-5, 1981.

52. Brenner, D. J., Prael, R. E., Private Communication, Dec. 1981.

53. Brenner, D., private communication, Oct. 20, 1982.

54. Dimbylow, P. J., Neutron Cross-sections and Kerma Values for Carbon, Nitrogen and Oxygen from 20 to 50 MeV, Phys. Med. Biol. 25, 637 (1980).

55. Dimbylow, P. J., Neutron Cross-Sections and Kerma Values for Elements of Biological Importance from 20 to 50 MeV. Proc. 4th Symp. Neutron Dosimetry in Biology and Medicine, June 1-5, 1981, Munich.

56. Dimbylow, P. J., Neutron Cross-Section and Kerma value Calculations for C, N, O, Mg, Al, P, S, Ar and Ca from 20 to 50 MeV, Phys. Med. Biol. 27, 989 (1982).

57. Dimbylow, P. J., Private communication, Sept. 29, 1982.

58. Wells, A. H., A Consistent Set of Kerma Values for H, C, N, and O for Neutrons of Energies from 10 to 80 MeV, Radiat. Res. 80, 1 (1979).

59. Herling, G. H., Bassel, R. H., Adams, J. H., Fraser, W. A., Neutron Induced Reactions in Tissue-Resident Elements, Washington DC: Naval Research Laboratory Report 8441, July 8, 1981.

60. Brady, F. P., Romero, J. L., Neutron Induced Reactions in Tissue Resident Elements, Final Report to the National Cancer Institute, Davis: University of California, 1979.

61. J. J. Coyne, private communication.

62. Control Data Corporation, Minneapolis, Minnesota.

63. Rossi, H. H., and Failla, G., Tissue-Equivalent Ionization Chambers, Nucleonics 14, 32 (1956).

64. Frigerio, N. A., Coley, R. F., Sampson, M. J., Depth Dose Determination I. Tissue-equivalent Liquids for Standard Man and Muscle, Phys. Med. Biol. 17, 792 (1972).

65. AAPM Report No. 7, Protocol for Neutron Beam Dosimetry, New York: American Institute of Physics, 1980.

66. Broerse, J. J., Mijnheer, B. J., Williams, J. R., European Protocol for Neutron Dosimetry for External Beam Therapy, Brit. J. Radiol. 54, 882 (1981).

Table Captions

Table I Fractional Mass Composition of Tissues and Materials.

Notes:

(a) Unless otherwise noted, all tissue compositions are derived from ICRP 23.[4] Numbers in parentheses denote organ or tissue number in Table 108 of above reference. Nine trace elements are included in "others", if present: F, Na, Mg, P, S, Cl, Ar, K and Ca. Mass fractions for trace elements exceeding 1% are listed explicitly as percentages.

Table II Variations in Composition of Some Tissues and Materials.

Notes:

(a) Eight trace elements are included in "others", if present: F, Na, Mg, P, S, Cl, K and Ca. Mass fractions for trace elements exceeding 1% are listed explicitly as percentages.

(b) Relative abundances of trace elements derived from ICRP 23.[4]

(c) Tissue number 77 in Table 108.

(d) From Table IV; Ca added to achieve unity in sum of mass fractions.

(e) Compact femur.

(f) From Table IV.

(g) Mouse metaphyseal bone.

(h) Cortical bone (Tissue number 90 in Table 108).

(i) Human cortical bone.

(j) Recommended composition.

(k) Design goal.

(l) Measured composition.

Table III Comparison of Measured and Calculated Neutron Kermas[a]

Notes:

(a) In units of 10^{-15} J kg^{-1} m^2 n^{-1}.

(b) Results of weighted deviation algorithm. See text.

(c) Measured values corrected for detector threshold and heavy ion recoil energy.[60]

Table IV. Combinations of Elemental Kerma Functions Used in This Study.

Key: Al = Alsmiller et al.[48]

Be = Behrooz et al.[50]

Br = Brenner et al.[53]

Di = Dimbylow[56,57]

FB = Fleming[46] (<30 MeV); Bassel et al.[47] (>30 MeV)

We = Wells[58]

Notes:

(a) EX = change-over energy from kerma functions of Caswell et al.[45] to those listed in the Table.

(b) For combinations IX - XVI, EX = 20 MeV was used because Alsmiller et al.[48] did not calculate kerma functions below 20 MeV.

Table V Ratios of Average Kermas Calculated Using Variations in Elemental Compositions.(a)

Notes:

(a) All values are given as ratios: $(\bar{K}_t/\bar{K}_m) \times 100$.

(b) For details of different compositions, see Table II.

Table VI Summary of Differences in Kerma Ratios Due to Variations in Elemental Compositions.(a)

Notes:

(a) In each matrix box, on left hand side are extreme differences $+\Delta_+$ and $-\Delta_-$ from reference kerma ratios given in Table V; on right hand side is r.m.s. deviation $\pm\sigma_\alpha$, calculated from Equation 5 in the text.

(b) Chosen reference compositions are used in all subsequent Tables.

Table VII Average Kermas and Kerma Ratios Calculated Using Variations in Energy Spectra.

Notes:

(a) Details of spectral variations are discussed in the text.

(b) Values for average muscle kerma, K_m, are given in units of 10^{-15} J kg^{-1} m^2 n^{-1}. Values for other materials are given as kerma ratios: $(K_t/\bar{K}_m) \times 100$.

Table VIII Summary of Differences in Average Kermas and Kerma Ratios due to Variations in Energy Spectra.

Notes:

(a) Extreme differences from reference values $+\Delta_+$ and $-\Delta_-$ (L.H.S.) and $\pm\sigma_N$ (R.H.S.) are in percent for muscle, in units of $(\bar{K}_t/\bar{K}_m) \times 100$ for other substances. σ_N are r.m.s. deviations from the reference, calculated from Eq. 5 in the text.

(b) Upper figure is difference between $\bar{K}_m$ or kerma ratios k_t for monochromatic beam and mean $\bar{K}_m$ or k_t for the three depths. Lower ($\pm$) figure is standard deviation of $\bar{K}_m$ or k_t for the three depths. Upper figure is taken as σ_N when combining uncertainties.

Table IX Average Kermas and Kerma Ratios Calculated Using Various Kerma Function Combinations for:

(a) p(66)Be neutron beam.

(b) p(41)Be neutron beam.

(c) d(50)Be neutron beam.

(d) d+various neutron beams.

Notes to all Tables IX (a)-(d).

(a) Details of kerma function combinations are given in Table IV.

(b) Values for average muscle kerma, $\bar{K}_m$, are given in units of 10^{-15} J kg^{-1} m^2 n^{-1}. Values for other substances are given as ratios: $(\bar{K}_t/\bar{K}_m) \times 100$.

Table X Summary of Differences in Average Kermas and Kerma Ratios due to Various Kerma Function Combinations.

Notes:

(a) Extreme differences from reference values $+\Delta_+$ and $-\Delta_-$ (L.H.S.) and $\pm\sigma_K$ (R.H.S.) are in percent for muscle, in units of $(\bar{K}_t/\bar{K}_m) \times 100$ for other substances. σ_K are r.m.s. deviations from the reference, calculated from Eq. 5 in the text.

Table XI Summary of Reference Average Kermas and Kerma Ratios, Uncertainties, and Hydrogen Partial Kermas.

Key for each matrix box:

Upper figure is average reference kerma, in units of 10^{-15} J kg^{-1} m^2 n^{-1} for muscle ($\bar{K}_m$), or kerma ratios: 100 x ($\bar{K}_t/\bar{K}_m$) for all other substances.

Middle ($\pm$) figure is total uncertainty calculated from Eq. 6 in the text, in percent for muscle and in units of 100 x ($\bar{K}_t/\bar{K}_m$) for all other substances.

Lower figure, in parentheses, is percentage of average kerma due to hydrogen.

Notes on combinations of uncertainties.

Subscripts α, K, and N to σ_i refer to partial uncertainties due to variations in elemental composition, kerma functions and neutron energy spectrum, respectively. $\sigma_{\alpha M}$ is composition uncertainty in muscle average kerma.

(a) All partial σ_i calculated.

(b) σ_K and σ_N calculated; $\sigma_\alpha=\sigma_\alpha(A-150)$.

(c) σ_K and σ_N calculated; $\sigma_\alpha=0$.

(d) $\sigma^2 = \sigma_{\alpha M}^2 + \sigma_K^2$ (water) $+\sigma_N^2$ (water) $+ \sigma_{\alpha M}^2$.

(e) $\sigma^2 = \sigma_{\alpha M}^2 + \sigma_K^2$ (fat) $+ \sigma_N^2$ (fat) $+ \sigma_{\alpha M}^2$.

(f) $\sigma = \sigma(A-150)$.

(g) $\sigma^2 = \sigma_\alpha^2(A-150) + \sigma_{\alpha M}^2$.

Table XII Comparison of Quoted Kerma Ratios of A-150 T.E. Plastic Relative to Muscle.

Notes:

(a) No uncertainties quoted.

(b) ±2% uncertainties quoted for all beams.

(c) Unassigned range of values; uncertainties quoted as from +2.6% for the d(16)Be beam to ±9.7% for the p(66)Be beam.

Table I

Fractional Mass Composition of Tissues and Materials

Material	H	C	N	O	Others	$\sum\alpha_j$	Notes (a)
Muscle (ICRU)	.102	.123	.035	.729	.011	1.000	S+K+P+Na+Mg+Ca
Skin	.100	.227	.046	.615	.006	.994	(96)
Whole Blood	.100	.098	.029	.745	.008	.981	(10)
Brain	.108	.133	.012	.725	.010	.992	(29)
Fat	.116	.640	.008	.227	.003	.994	(3)
Yellow Marrow	.113	.633	.006	.227	.003	.982	(93)
Red Marrow	.100	.413	.032	.413	.000	.959	(92)
Intestine	.100	.094	.021	.770	.006	.991	(43)
Kidneys	.103	.129	.027	.742	.008	1.010	(64)
Liver	.100	.144	.028	.667	.011	.951	(66)
Pancreas	.097	.130	.021	.670	.008	.926	(79)
Lungs	.099	.100	.028	.740	.009	.976	(67)
Bone (ICRU)	.064	.278	.027	.410	.221	1.000	14.7 Ca, 7.0 P, Mg+S
A-150	.102	.768	.036	.059	.035	1.000	1.7 F, 1.8 Ca.[15]
Polyethylene	.144	.856	.000	.000	.000	1.000	
Polystyrene	.077	.923	.000	.000	.000	1.000	
Nylon	.098	.637	.124	.141	.000	1.000	Type 6/6
Lucite	.080	.600	.000	.320	.000	1.000	
Mylar	.042	.625	.000	.333	.000	1.000	
T.E. Solution	.102	.120	.035	.743	.000	1.000	Ref. 64
T.E. Gas	.102	.456	.035	.407	.000	1.000	Ref. 63
Air (Dry)	.000	.000	.755	.232	.013	1.000	1.3 Ar

Table II

Variations in Composition of Some Tissues and Materials

Material		Ref.	H	C	N	O	Others	$\sum \alpha_j$	Notes [a]
Muscle	A	(5)	.102	.123	.035	.729	.011	1.000	(b)
	B	(4)	.100	.107	.028	.750	.009	.994	(c)
	C	(11)	.100	.117	.033	.750	.000	1.000	
Bone	A	(7)	.073	.280	.029	.320	.298	1.000	22.4 Ca, 7.0 P (d)
	B	(5)	.064	.278	.027	.410	.221	1.000	14.7 Ca, 7.0 P (e)
	C	(7)	.056	.093	.033	.394	.424	1.000	28.0 Ca, 13.4 P (f)
	D	(12)	.056	.124	.038	.547	.235	1.000	16.0 Ca, 7.1 P (g)
	E	(4)	.045	.138	.040	.425	.305	.953	20.0 Ca, 10.0 P (h)
	F	(13)	.034	.155	.040	.441	.330	1.000	22.2 Ca, 10.2 P (i)
Fat	A	(4)	.116	.640	.008	.227	.003	.994	Subcutaneous
	B	(11)	.115	.602	.000	.283	.000	1.000	From Rat
	C	(14)	.124	.768	.000	.108	.000	1.000	Tristearin
A-150	A	(15)	.102	.768	.036	.059	.035	1.000	1.7 F, 1.8 Ca (j)
	B	(16)	.101	.776	.035	.052	.036	1.000	1.7 F, 1.8 Ca (k)
	C	(16)	.103	.770	.033	.069	.025	1.000	1.1 F, 1.4 Ca (l)
Nylon	A	(5)	.098	.637	.124	.141	.000	1.000	Type 6/6
	B	(5)	.107	.681	.099	.113	.000	1.000	Type 6/10
	C	(5)	.104	.648	.100	.148	.000	1.000	Zytel 69

Table III

Comparison of Measured and Calculated Neutron Kermas[a]

Element	C				N				O			
Energy (MeV)	27.4	39.7	60.7	$\sum$[b]	27.4	39.7	60.7	$\sum$[b]	27.4	39.7	60.7	$\sum$[b]
	MEASURED[c]											
Brady et al.[60]	4.0	4.1	5.6	-	3.0	4.2	6.1	-	2.3	3.0	5.1	-
	CALCULATED											
Alsmiller et al.[48]	3.4	4.3	5.7	0.9	.23	3.2	5.0	2.8	2.2	3.1	4.2	1.1
Behrooz et al.[50]	3.2	3.7	6.5	2.1	2.8	3.9	6.2	0.6	2.8	3.4	4.5	1.5
Behrooz et al.[49]	3.2	3.8	6.3	-	2.8	3.9	6.2	-	2.6	3.3	4.6	-
Brenner et al.[53]	3.3	3.8	4.7	2.0	3.2	4.1	5.0	1.4	2.9	3.6	4.5	1.8
Brenner et al.[51,52]	3.4	3.8	4.6	-	3.4	4.3	4.9	-	2.6	3.2	4.4	-
Dimbylow[56]	3.7	4.2	5.4	0.6	3.8	5.0	6.6	2.1	2.4	3.3	4.4	1.1
Dimbylow[54]	4.6	5.5	-	-	3.7	5.0	-	-	2.8	3.6	-	-
Wells[58]	3.9	4.1	4.7	1.0	3.7	4.7	6.1	1.2	2.4	3.0	4.2	1.0

Notes:
(a) In units of 10^{-15} J kg^{-1} m^2 n^{-1}
(b) Results of weighted deviation algorithm. See text.
(c) Measured values corrected for detector threshold and heavy ion recoil energy.[60]

Table IV

Combinations of Elemental Kerma Functions

Used in This Study

Kerma Comb.	EX[a] (MeV)	H	C	N	O	Notes
I	15	Be	Di	Be	We	Reference Set
II	20	Al	Al	Al	Al	Other Recent Sources
III	15	Be	Be	Be	Be	
IV	15	Be	Br	Br	Br	
V	10	FB	Di	Di	Di	
VI	10	We	We	We	We	
VII	20	Be	Di	Be	We	Different Change-Over Energies
VIII	30	Be	Di	Be	We	for Reference Set
						Extreme Kerma Functions [b]
IX	20	Al	Di	Be	We	Highest H
X	20	FB	Di	Be	We	Lowest H
XI	20	Be	Al	Be	We	Highest C
XII	20	Be	Be	Be	We	Lowest C
XIII	20	Be	Di	Di	We	Highest N
XIV	20	Be	Di	Al	We	Lowest N
XV	20	Be	Di	Be	Br	Highest O
XVI	20	Be	Di	Be	Al	Lowest O

Table V

Ratios of Average Kerma Calculated Using Variations in Elemental Compositions[a]

Materials[b]		p(66)Be	p(41)Be	d(50)Be	d(22)Be	d(16)Be	d+T	d(8.3)D
Muscle	A	100.0	100.0	100.0	100.0	100.0	100.0	100.0
	B	98.5	98.4	98.4	98.4	98.3	98.5	98.3
	C	98.7	98.5	98.6	98.5	98.4	98.8	98.4
Bone	A	84.6	81.2	82.0	77.5	76.3	78.9	77.0
	B	78.8	74.7	75.7	70.4	68.8	73.3	69.4
	C	71.7	66.9	67.5	63.1	61.4	64.8	62.5
	D	72.1	67.5	68.3	63.8	62.0	67.0	62.8
	E	65.6	59.8	60.8	55.0	52.8	58.9	53.8
	F	59.0	52.2	53.3	46.3	43.7	51.2	44.9
Fat	A	115.3	115.9	116.6	112.9	113.1	113.0	112.6
	B	113.6	114.2	114.9	111.4	111.5	111.6	111.1
	C	121.2	122.4	123.2	118.9	119.3	118.6	118.6
A-150	A	108.2	107.2	108.4	102.0	101.5	104.0	101.1
	B	108.0	106.8	108.1	101.6	101.0	103.6	100.6
	C	109.0	108.1	109.3	103.1	102.6	104.9	102.2
Nylon	A	105.2	103.6	104.6	99.2	98.7	101.3	98.2
	B	111.0	110.3	111.2	106.2	106.0	107.5	105.4
	C	108.7	107.8	108.6	103.7	103.4	105.2	102.9

Table VI

Summary of Differences in Kerma Ratios due to Variations in Elemental Compositions[a]

BEAM	MUSCLE	BONE	FAT	A-150	NYLON
p(66)Be	+0 ±1.4 -1.5	+19.0 ±11.5 -6.6	+5.9 ±4.3 -1.7	+0.8 ±0.6 -0.2	+2.3 ±3.0 -3.5
p(41)Be	+0 ±1.6 -1.6	+21.4 ±13.0 -7.6	+6.5 ±4.8 -1.7	+0.9 ±0.7 -0.4	+2.5 ±3.5 -4.2
d(50)Be	+0 ±1.5 -1.6	+21.2 ±12.9 -7.5	+6.6 ±4.8 -1.7	+0.9 ±0.7 -0.3	+2.6 ±3.4 -4.0
d(22)Be	+0 ±1.6 -1.6	+22.5 ±13.9 -8.7	+6.0 ±4.4 -1.5	+1.1 ±0.8 -0.4	+2.5 ±3.6 -4.5
d(1.6)Be	+0 ±1.6 -1.7	+23.5 ±14.5 -9.1	+6.2 ±4.5 -1.6	+1.1 ±0.8 -0.5	+2.6 ±3.8 -4.7
d+T	+0 ±1.4 -1.5	+20.0 ±12.4 -7.7	+5.6 ±4.1 -1.4	+0.9 ±0.7 -0.4	+2.3 ±3.2 -3.9
d(8.3)d	+0 ±1.6 -1.7	+23.2 ±14.3 -8.9	+6.0 ±4.4 -1.5	+1.1 ±0.8 -0.5	+2.5 ±3.8 -4.7
Ref. Comp.[b]	A(ICRU)	E(ICRP)	A(ICRP)	A(Ref. 15)	C(Zytel 69)

Table VII

Average Kermas and Kerma Ratios Calculated Using Variations in Energy Spectra

Spectral Variations (a)	MUSCLE (ICRU) (b)	A-150 (Ref.15)	BONE (ICRP)	FAT (ICRP)	WATER (H_2O)	POLYETH. $(CH_2)_n$	POLYSTYR. $(CH)_n$	NYLON (Zytel 6
p(66)Be Ref	6.227	108.2	65.6	115.3	104.0	134.4	94.7	108.7
Var. (i)	6.439	108.5	66.2	115.3	103.9	134.2	95.3	108.9
Var. (ii)	5.887	107.8	64.3	115.3	104.3	134.8	93.7	108.4
Var. (iii)	5.664	108.1	65.2	115.3	104.1	134.5	94.4	108.6
Var. (iv)	6.689	108.8	67.0	115.3	103.7	134.0	95.9	109.1
p(41)Be Ref	5.584	107.2	59.8	115.9	105.3	137.2	91.3	107.8
Var. (i)	5.794	107.5	60.5	116.0	105.1	137.1	92.0	108.0
Var. (ii)	5.194	106.6	58.6	115.8	105.6	137.4	90.1	107.4
Var. (iii)	4.848	107.0	59.3	115.9	105.5	137.3	90.9	107.6
Var. (iv)	6.114	107.9	61.4	116.1	104.9	136.9	92.9	108.3
Var. (v)	4.323	106.2	58.1	115.6	105.8	137.2	89.7	107.0
d(50)Be Ref	5.984	108.4	60.8	116.6	105.0	137.8	93.3	108.6
Var. (i)	5.797	108.3	60.7	116.6	105.0	137.7	93.1	108.6
Var. (ii)	6.377	108.8	61.7	116.8	104.7	137.7	94.1	109.0
d(16)Be Ref	4.334	101.5	52.8	113.1	107.6	135.7	81.5	103.4
Var. (i)	4.114	101.5	52.7	113.1	107.6	135.7	81.4	103.4
Var. (ii)	4.858	101.4	53.5	112.8	107.5	135.0	81.6	103.3
d+T monochr	6.733	104.0	58.9	113.0	105.8	132.3	88.4	105.2
2cm deep	5.176	105.0	56.4	114.7	106.2	136.3	87.8	106.1
7cm deep	5.088	104.6	56.1	114.6	106.3	136.2	87.2	105.9
17cm deep	5.006	104.2	55.9	114.3	106.4	135.9	86.6	105.5

Table VIII

Summary of Differences in Average Kermas and Kerma Ratios

due to Variations in Energy Spectra

BEAM	MUSCLE (ICRU) (a)	A-150 (Ref.15)	BONE (ICRP)	FAT (ICRP)	WATER (H_2O)	POLYETH. $(CH_2)_n$	POLYSTYR. $(CH)_n$	NYLON (Zytel
p(66)Be	+7.4% ±6.7% -9.0%	+0.6 ±0.4 -0.4	+1.4 ±1.0 -1.3	+0 ±0 -0	+0.3 ±0.2 -0.3	+0.4 ±0.3 -0.4	+1.2 ±0.8 -1.0	+0.4 ±0. -0.3
p(41)Be	+10.2% ±12.7% -22.1%	+0.7 ±0.6 -1.0	+1.6 ±1.2 -1.7	+0.2 ±0.2 -0.3	+0.5 ±0.3 -0.4	+0.2 ±0.2 -0.3	+1.6 ±1.2 -1.6	+0.5 ±0. -0.8
d(50)Be	+6.6% ±5.1% -3.1%	+0.4 ±0.3 -0.1	+0.9 ±0.6 -0.1	+0.2 ±0.1 -0	+0 ±0.2 -0.3	+0 ±0.1 -0.1	+0.8 ±0.6 -0.2	+0.4 ±0. -0
d(16)Be	+12.1% ±9.3% -5.1%	+0 ±0.1 -0.1	+0.7 ±0.5 -0.1	+0 ±0.2 -0.3	+0 ±0.1 -0.1	+0 ±0.5 -0.7	+0.1 ±0.1 -0.1	+0 ±0. -0.1
d+T(b)	-24.4% ±1.3%	+0.6 ±0.4	-2.8 ±0.3	+1.5 ±0.2	+0.5 ±0.1	+3.8 ±0.2	-1.2 ±0.6	+0.6 ±0.3

Table IX (a)

Average Kermas and Kerma Ratios Calculated Using Various Kerma Function Combinations

p(66)Be

Kerma Combin. (a)	MUSCLE (ICRU) (b)	A-150 (Ref.15)	BONE (ICRP)	FAT (ICRP)	WATER (H_2O)	POLYETH. $(CH_2)_n$	POLYSTYR. $(CH)_n$	NYLON (Zytel
I	6.227	108.2	65.6	115.3	104.0	134.4	94.7	108.7
II	6.260	109.2	65.2	116.4	104.1	136.0	96.1	109.1
III	6.290	105.0	65.4	112.6	104.7	130.4	90.9	105.9
IV	6.381	102.5	65.3	110.6	105.2	127.3	88.3	103.7
V	6.268	107.9	65.8	114.6	103.8	133.3	94.1	108.9
VI	6.238	108.0	65.6	114.9	104.0	133.9	94.0	108.7
VII	6.257	108.1	65.5	115.2	104.0	134.2	94.7	108.6
VIII	6.311	108.6	65.4	115.5	103.9	134.5	95.5	109.2
IX	6.305	108.0	65.3	115.2	104.1	134.2	94.6	108.6
X	6.230	108.1	65.6	115.2	104.0	134.1	94.8	108.7
XI	6.265	108.7	65.5	115.7	103.9	134.8	95.5	109.1
XII	6.242	106.8	65.3	114.2	104.3	132.8	93.1	107.6
XIII	6.275	108.1	65.6	114.9	103.7	133.8	94.4	109.1
XIV	6.241	108.1	65.3	115.4	104.3	134.5	94.9	108.2
XV	6.442	105.3	65.4	112.8	104.5	130.3	92.0	106.1
XVI	6.221	108.6	65.5	115.7	103.9	134.9	95.2	109.1

Table IX (b)

Average Kermas and Kerma Ratios Calculated Using Various Kerma Function Combinations

p(41)Be

Kerma Combin. (a)	MUSCLE (ICRU) (b)	A-150 (Ref.15)	BONE (ICRP)	FAT (ICRP)	WATER (H_2O)	POLYETH. $(CH_2)_n$	POLYSTYR. $(CH)_n$	NYLON (Zytel
I	5.548	107.2	59.8	115.9	105.3	137.2	91.3	107.8
II	5.584	107.5	59.6	116.3	105.3	137.6	91.9	107.9
III	5.577	102.6	59.5	112.2	106.2	131.8	85.8	103.9
IV	5.666	102.9	59.8	112.3	106.0	131.7	86.6	104.3
V	5.579	107.3	60.1	115.7	105.0	136.9	91.3	108.3
VI	5.517	108.7	60.1	116.9	104.8	138.6	92.9	109.3
VII	5.592	107.0	59.7	115.7	105.3	136.8	91.3	107.7
VIII	5.678	107.8	59.7	116.3	105.0	137.2	92.7	108.5
IX	5.603	107.0	59.7	115.7	105.3	136.8	91.3	107.7
X	5.580	107.0	59.7	115.7	105.3	136.8	91.3	107.7
XI	5.595	107.2	59.7	115.9	105.2	137.0	91.6	107.9
XII	5.568	104.7	59.5	114.0	105.8	134.4	88.4	105.9
XIII	5.604	107.0	59.8	115.5	105.1	136.5	91.1	108.1
XIV	5.587	107.0	59.6	115.8	105.4	136.9	91.4	107.5
XV	5.717	104.9	59.8	113.9	105.7	133.8	89.3	105.8
XVI	5.577	107.3	59.7	116.0	105.2	137.2	91.6	107.9

Table IX (c)

Average Kermas and Kerma Ratios Calculated Using
Various Kerma Function Combinations

d(50)Be

Kerma Combin. (a)	MUSCLE (ICRU) (b)	A-150 (Ref.15)	BONE (ICRP)	FAT (ICRP)	WATER (H_2O)	POLYETH. $(CH_2)_n$	POLYSTYR. $(CH)_n$	NYLON (Zytel
I	5.984	108.4	60.8	116.6	105.0	137.8	93.3	108.6
II	6.088	108.3	60.5	116.6	104.9	137.4	93.8	108.5
III	5.976	102.5	60.3	111.9	106.1	131.1	86.0	103.8
IV	6.108	103.3	60.7	112.3	105.8	131.4	87.4	104.4
V	5.990	108.9	61.0	116.8	104.6	138.0	93.6	109.6
VI	5.952	110.5	61.2	118.1	104.3	139.9	95.7	110.8
VII	6.090	108.0	60.5	116.2	104.9	136.9	93.3	108.4
VIII	6.238	108.9	60.4	116.7	104.6	137.1	94.9	109.4
IX	6.098	107.9	60.5	116.2	104.9	136.9	93.2	108.4
X	6.077	108.0	60.5	116.2	104.9	136.9	93.3	108.4
XI	6.093	108.2	60.5	116.4	104.9	137.1	93.6	108.6
XII	6.060	105.4	60.2	114.2	105.4	134.1	90.0	106.3
XIII	6.102	107.9	60.6	116.0	104.7	136.6	93.1	108.8
XIV	6.084	108.0	60.5	116.3	105.0	137.0	93.3	108.2
XV	6.214	106.0	60.6	114.5	105.2	134.1	91.4	106.6
XVI	6.082	108.1	60.5	116.3	104.9	137.0	93.4	108.5

Table IX (d)

Average Kermas and Kerma Ratios Calculated Using Various Kerma Function Combinations

Kerma Combin. (a)	MUSCLE (ICRU) (b)	A-150 (Ref.15)	BONE (ICRP)	FAT (ICRP)	WATER (H_2O)	POLYETH. $(CH_2)_n$	POLYSTYR. $(CH)_n$	NYLC (Zytel
	d(22)Be							
I	5.331	102.0	55.0	112.9	107.1	134.5	83.1	103.7
II	5.360	102.0	55.0	112.8	107.1	134.3	83.3	103.7
III & VII	5.325	101.2	54.9	112.2	107.3	133.5	82.0	103.0
IV	5.335	101.5	55.0	112.5	107.2	133.9	82.5	103.3
V	5.373	102.6	55.2	113.3	106.9	134.9	83.8	104.3
VI	5.259	103.0	55.1	113.8	107.0	135.9	84.2	104.5
	d(16)Be							
I	4.334	101.5	52.8	113.1	107.6	135.7	81.5	103.4
V	4.364	101.8	53.0	113.3	107.5	135.8	81.9	103.7
VI	4.301	102.1	52.8	113.7	107.5	136.5	82.1	103.9
	d+T							
I	6.733	104.0	58.9	113.0	105.8	132.3	88.4	105.2
V	6.389	109.7	59.3	118.0	104.8	140.4	93.9	110.5
VI	6.348	106.2	59.4	115.2	105.6	136.1	90.4	107.0
	d(8.3)D							
I	5.162	101.1	53.8	112.6	107.7	134.7	81.3	102.9
V	5.286	100.9	54.2	112.2	107.5	133.8	81.3	102.8
VI	5.121	102.0	53.9	113.4	107.5	135.9	82.1	103.6

Table X

Summary of Differences in Average Kermas and Kerma Ratios due to Various Kerma Function Combinations[a]

BEAM	MUSCLE (ICRU)	A-150 (Ref.15)	BONE (ICRP)	FAT (ICRP)	WATER (H_2O)	POLYETH. $(CH_2)_n$	POLYSTYR. $(CH)_n$	NYLON (Zytel
p(66)Be	+3.5% ±1.3% -0.1%	+1.0 ±2.5 -5.7	+0.2 ±0.2 -0.4	+1.1 ±2.0 -4.7	+1.2 ±0.5 -0.3	+1.6 ±3.2 -7.1	+1.4 ±2.9 -6.4	+0.5 ±2. -5.0
p(41)Be	+3.0% ±1.3% -0.6%	+1.5 ±2.5 -4.6	+0.3 ±0.2 -0.3	+1.0 ±2.0 -3.7	+0.9 ±0.5 -0.5	+1.4 ±3.0 -5.5	+1.6 ±2.9 -5.5	+1.5 ±2. -3.9
d(50)Be	+4.0% ±2.1% -0.5%	+2.1 ±3.1 -5.9	+0.4 ±0.3 -0.5	+1.5 ±2.5 -4.7	+1.1 ±0.6 -0.7	+2.1 ±3.6 -6.7	+2.4 ±3.7 -7.3	+2.2 ±2. -4.8
d(22)Be	+0.8% ±0.7% -1.4%	+1.0 ±0.7 -0.8	+0.2 ±0.1 -0.1	+0.9 ±0.6 -0.7	+0.2 ±0.1 -0.2	+1.4 ±0.8 -1.0	+1.1 ±0.8 -1.1	+0.8 ±0. -0.7
d(16)Be	+0.7% ±0.7% -0.8%	+0.6 ±0.5 -0	+0.2 ±0.1 -0	+0.6 ±0.4 -0	+0 ±0.1 -0.1	+0.8 ±0.6 -0	+0.6 ±0.5 -0	+0.5 ±0. -0
d+T	+0 ±5.4% -5.7%	+5.7 ±4.3 -0	+0.5 ±0.5 -0	+5.0 ±3.9 -0	+0 ±0.7 -1.0	+8.1 ±6.3 -0	+5.5 ±4.1 -0	+5.3 ±4. -0
d(8.3)D	+2.4% ±1.8% -0.8%	+0.9 ±0.7 -0.2	+0.4 ±0.3 -0	+0.8 ±0.6 -0.4	+0 ±0.2 -0.2	+1.2 ±1.1 -0.9	+0.8 ±0.6 -0.	+0.7 ±0. -0.1

Table XI

Summary of Reference Average Kermas and Kerma Ratios, Uncertainties, and Hydrogen Partial Kermas

MATERIAL	p(66)Be	p(41)Be	d(50)Be	d(22)Be	d(16)Be	d+T	d(8.3)D	Notes
MUSCLE (ICRU)	6.2(3) ±7% (66)	5.5(5) ±13% (75)	5.9(8) ±6% (73)	5.3(3) ±7% (81)	4.3(3) ±10% (85)	6.7(3) ±25% (71)	5.1(6) ±8% (84)	(a)
SKIN	100 ±2 (65)	100 ±2 (73)	100 ±2 (72)	99 ±2 (81)	99 ±2 (85)	99 ±2 (70)	99 ±2 (84)	(d)
WHOLE BLOOD	98 ±2 (66)	98 ±2 (74)	98 ±2 (73)	98 ±2 (81)	98 ±2 (85)	98 ±2 (71)	98 ±2 (84)	(d)
BRAIN	104 ±3 (68)	104 ±3 (76)	104 ±3 (74)	105 ±2 (83)	105 ±2 (86)	104 ±5 (73)	105 ±2 (85)	(e)
FAT (ICRP)	115 ±5 (66)	116 ±5 (74)	117 ±6 (71)	113 ±5 (83)	113 ±5 (86)	113 ±6 (72)	113 ±5 (86)	(a)
YELLOW MARROW	113 ±3 (65)	113 ±3 (73)	114 ±3 (71)	110 ±2 (82)	110 ±2 (86)	111 ±5 (72)	110 ±2 (85)	(e)
RED MARROW	102 ±2 (63)	102 ±2 (72)	102 ±2 (70)	99 ±2 (80)	99 ±2 (84)	101 ±2 (70)	99 ±2 (83)	(d)
INTESTINE	98 ±2 (66)	98 ±2 (74)	98 ±2 (73)	98 ±2 (81)	98 ±2 (85)	98 ±2 (71)	98 ±2 (84)	(d)
KIDNEYS	101 ±2 (66)	101 ±2 (75)	101 ±2 (73)	101 ±2 (82)	101 ±2 (85)	101 ±2 (72)	101 ±2 (84)	(d)

Table XI (cont. 1)

MATERIAL	p(66)Be	p(41)Be	d(50)Be	d(22)Be	d(16)Be	d+T	d(8.3)D	Notes
LIVER	99 ±2 (65)	99 ±2 (74)	99 ±2 (72)	98 ±2 (81)	98 ±2 (85)	99 ±2 (71)	98 ±2 (84)	(d)
PANCREAS	97 ±2 (65)	96 ±2 (74)	96 ±2 (72)	96 ±2 (81)	96 ±2 (85)	97 ±2 (70)	96 ±2 (83)	(d)
LUNGS	98 ±2 (66)	98 ±2 (74)	98 ±2 (72)	98 ±2 (81)	97 ±2 (85)	98 ±2 (71)	98 ±2 (84)	(d)
BONE (ICRP)	66 ±12 (44)	60 ±13 (55)	61 ±13 (53)	55 ±14 (65)	53 ±15 (71)	59 ±13 (53)	54 ±14 (69)	(a)
A-150 (Ref. 15)	108 ±3 (61)	107 ±3 (70)	108 ±4 (67)	102 ±2 (80)	102 ±2 (84)	104 ±5 (69)	101 ±2 (83)	(a)
POLYETH.	134 ±4 (69)	137 ±4 (76)	138 ±4 (74)	134 ±2 (85)	136 ±2 (89)	132 ±8 (76)	135 ±2 (88)	(b)
POLYSTYR.	95 ±3 (53)	91 ±4 (62)	93 ±4 (59)	83 ±2 (74)	82 ±2 (79)	88 ±5 (61)	81 ±2 (78)	(b)
NYLON (Zytel 69)	109 ±4 (62)	108 ±4 (71)	108 ±5 (68)	104 ±4 (80)	103 ±4 (84)	105 ±5 (69)	103 ±4 (83)	(a)
LUCITE	93 ±3 (56)	90 ±3 (65)	91 ±4 (63)	85 ±2 (76)	83 ±2 (81)	88 ±5 (64)	83 ±2 (80)	(f)

Table XI (cont. 2)

MATERIAL	p(66)Be	p(41)Be	d(50)Be	d(22)Be	d(16)Be	d+T	d(8.3)D	Notes
MYLAR	69 ±3 (39)	63 ±3 (49)	65 ±4 (46)	55 ±2 (61)	52 ±2 (68)	63 ±5 (47)	52 ±2 (66)	(f)
GRAPHITE	48 ±4 (0)	38 ±4 (0)	41 ±5 (0)	23 ±2 (0)	18 ±2 (0)	37 ±7 (0)	19 ±2 (0)	(c)
WATER	104 ±2 (70)	105 ±2 (78)	105 ±2 (76)	107 ±2 (83)	108 ±2 (87)	106 ±2 (74)	108 ±2 (86)	(c)
T.E. SOLUTION	100 ±1 (66)	100 ±2 (74)	100 ±2 (73)	100 ±2 (81)	100 ±2 (85)	100 ±2 (71)	100 ±2 (84)	(g)
T.E. GAS	104 ±3 (63)	104 ±3 (72)	104 ±4 (70)	101 ±2 (81)	101 ±2 (85)	102 ±5 (70)	100 ±2 (84)	(f)
AIR (DRY)	45 ±4 (0)	33 ±4 (0)	34 ±4 (0)	26 ±2 (0)	22 ±2 (0)	36 ±8 (0)	22 ±3 (0)	(c)

Table XII

Comparison of Quoted Kerma Ratios of A-150

T.E. Plastic Relative to Muscle

Neutron Beam	This Work	Bewley	Smith et al.	AAPM	ECNEU
p(66)Be	1.08 ±3%	1.09 ±11%	-	1.05	1.07
p(41)Be	1.07 ±3%	-	-	-	|
d(50)Be	1.08 ±4%	-	1.05	1.05	|
d(22)Be	1.02 ±2%	-	1.05	1.05	|
d(16)Be	1.02 ±2%	1.03 ±3%	1.05	-	|
d+T	1.04 ±5%	1.04 ±5%	-	-	1.03
d(8.3)D	1.01 ±2%	-	-	1.04	-
Refs.	-	3	34	65	66
Notes	-	-	(a)	(b)	(c)

Figure Captions

Fig. 1 Neutron energy spectra assumed for the p(66)Be and p(41)Be beams. Solid lines indicate the reference spectra. Broken lines represent spectral variations for the p(41)Be beam: (i) half the expected contribution due to the evaporation process; (ii) twice this contribution; (iii) an E^{-1} low energy extrapolation matched to the peak of the evaporation contribution and (iv) no evaporation contribution at all, corresponding to a heavily filtered beam. In addition, (v), the measured p(41)Be spectrum[25] (open circles) with an E^{-1} low energy extrapolation added (closed circles) is also shown.

Fig. 2 Neutron energy spectra assumed for the d(16)Be beam. The solid line represents the reference spectrum from Ref. 24, with an added exponential low energy extrapolation adapted from Greenwood et al.[36] The broken lines represent: (i) an E^{-1} low energy tail to the above, and (ii) the spectrum from Ref. 21, arbitrarily matched at the peak, with an added low energy extrapolation through the origin.

Fig. 3 Kerma functions for Hydrogen. Upper full range solid line (using L.H.S. scale) represents reference kerma function, with symbols from Caswell et al.[45] (Δ) and Behrooz et al.[50] (▲). Lower symbols represent ratios of other kerma functions used in the calculations relative to reference values (R.H.S. scale): Fleming[46] and Bassel et al.[47] (O), Wells[58] (□) and Alsmiller et al.[48] (———).

Fig. 4 Kerma functions for Carbon. Upper full range solid line (using L.H.S scale) represents reference kerma function, with symbols from Caswell et al.[45] (Δ) and Dimbylow[56] (O). Lower symbols represent ratios of other kerma functions used in the calculations relative to the reference values (R.H.S. scale): Behrooz et al.[50] (▲), Brenner et al.[53] (●), Wells[58] (□) and Alsmiller et al.[48] (———).

Fig. 5 Kerma functions for Nitrogen. Upper full range solid line (using L.H.S. scale) represents reference kerma function, with symbols from Caswell et al.[45] (Δ) and Behrooz et al.[50] (▲). Lower symbols represent ratios of other kerma functions used in the calculations relative to the reference values (R.H.S. scale): Brenner et al.[50] (●), Dimbylow[56] (O), Wells[58] (□) and Alsmiller et al.[48] (———).

Fig. 6 Kerma functions for Oxygen. Upper full range solid line (using L.H.S. scale) represents reference kerma function, with symbols from Caswell et al.[45] (Δ) and Wells[58] (□). Lower symbols represent ratios of other kerma functions used in the calculations relative to the reference values (R.H.S. scale): Behrooz et al.[50] (▲), Dimbylow[56] (O), Brenner et al.[53] (●) and Alsmiller et al.[48] (———).

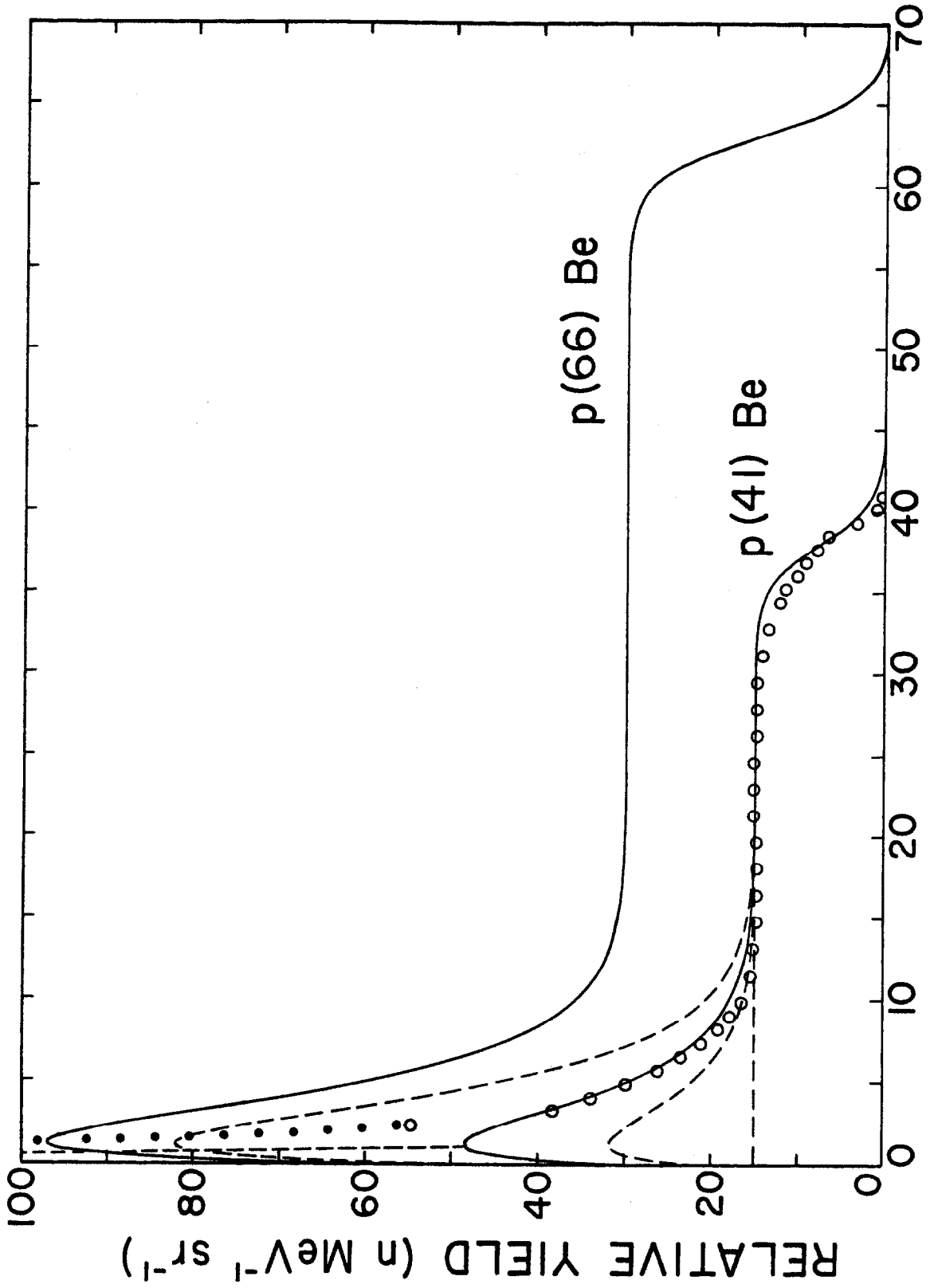
RELATIVE YIELD (n MeV⁻¹ sr⁻¹)
NEUTRON ENERGY (MeV)
p(66) Be
p(41) Be
0
20
40
60
80
100
10
30
50
70

Figure 1

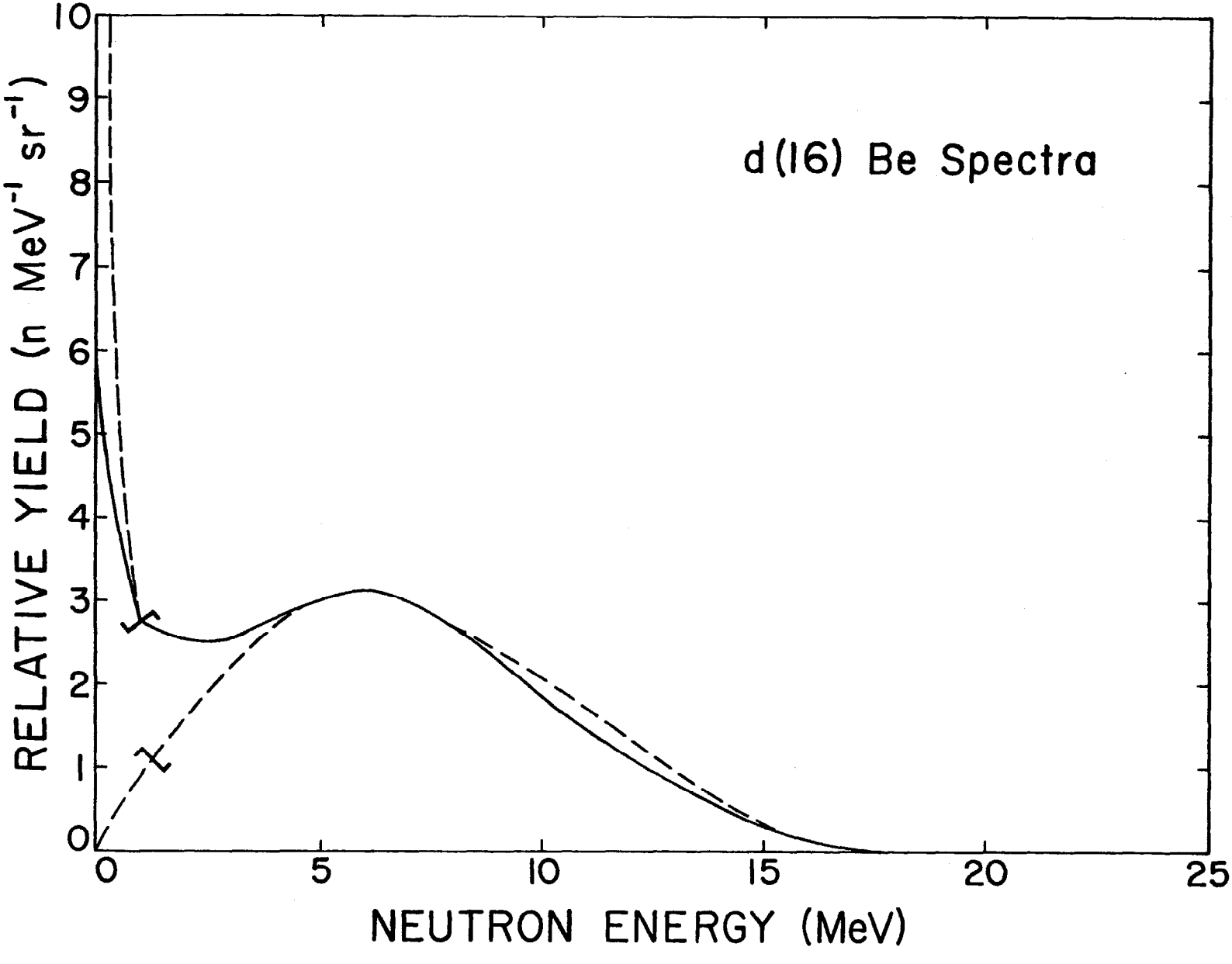
d(16) Be Spectra
RELATIVE YIELD (n MeV^{-1} sr^{-1})
NEUTRON ENERGY (MeV)
0
1
2
3
4
5
6
7
8
9
10
0
5
10
15
20
25

Figure 2

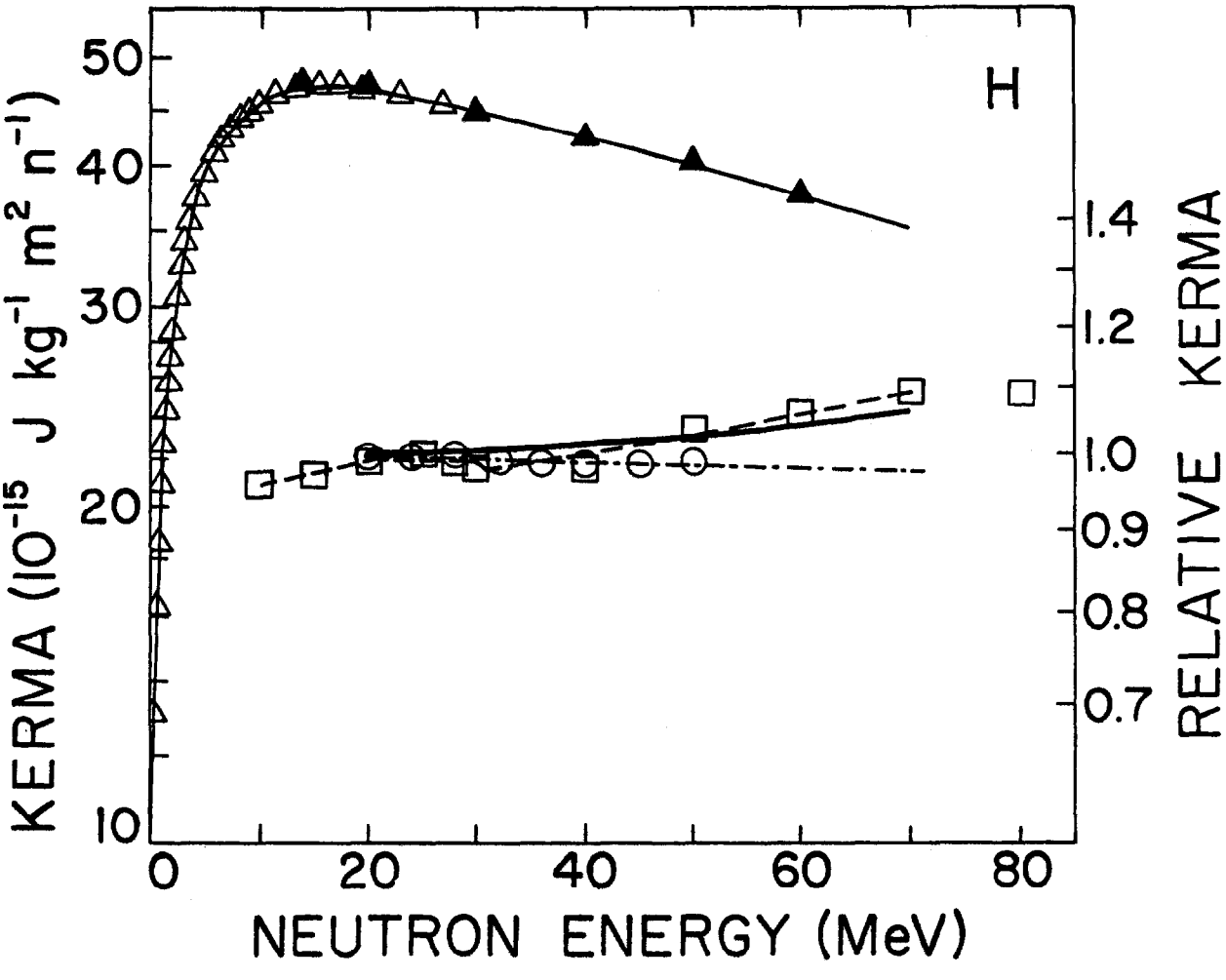

Figure 3

11-12-82

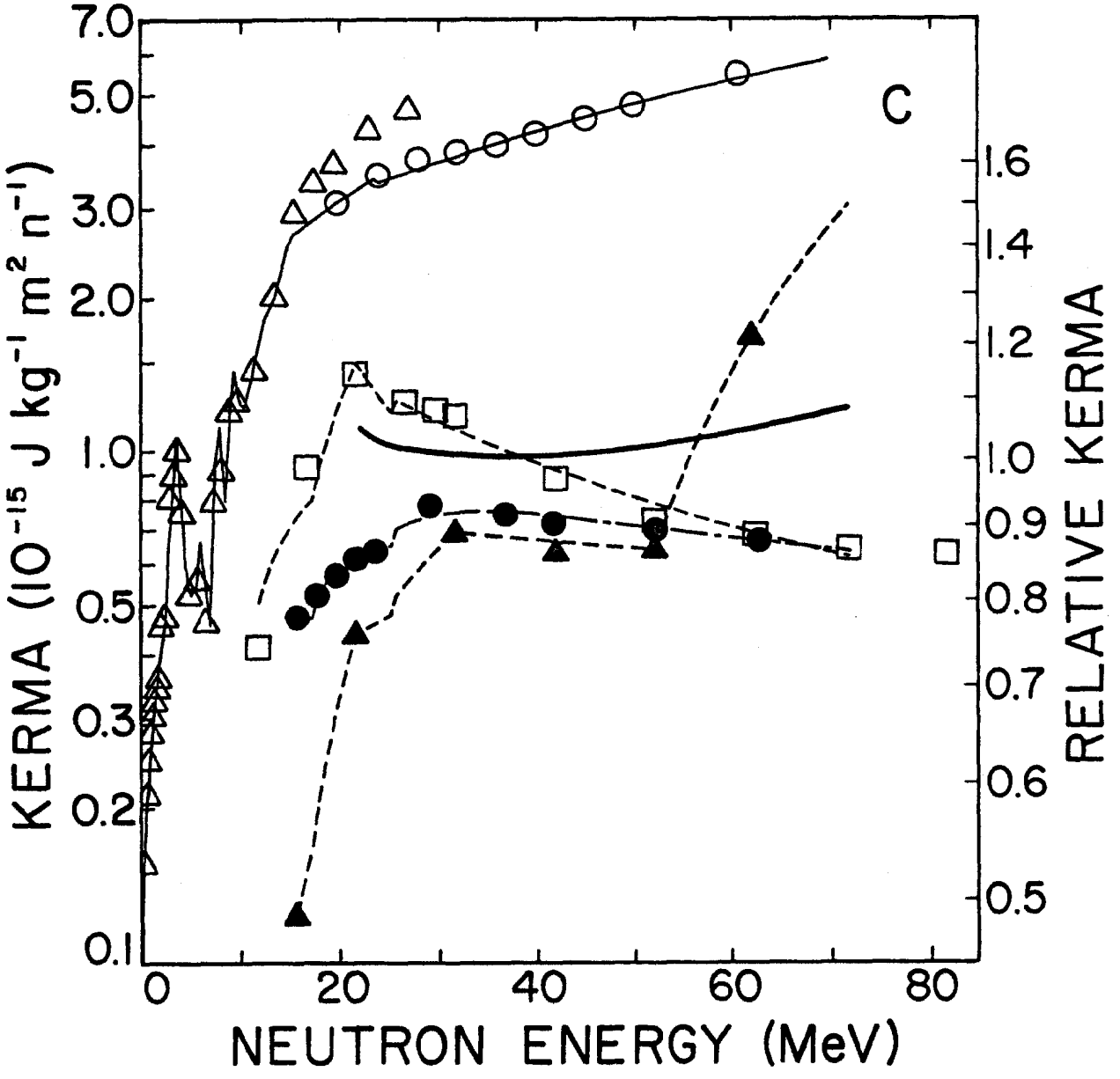
7.0
5.0
3.0
2.0
1.0
0.5
0.3
0.2
0.1
KERMA (10⁻¹⁵ J kg⁻¹ m² n⁻¹)
C
1.6
1.4
1.2
1.0
0.9
0.8
0.7
0.6
0.5
RELATIVE KERMA
0
20
40
60
80
NEUTRON ENERGY (MeV)

Figure 4

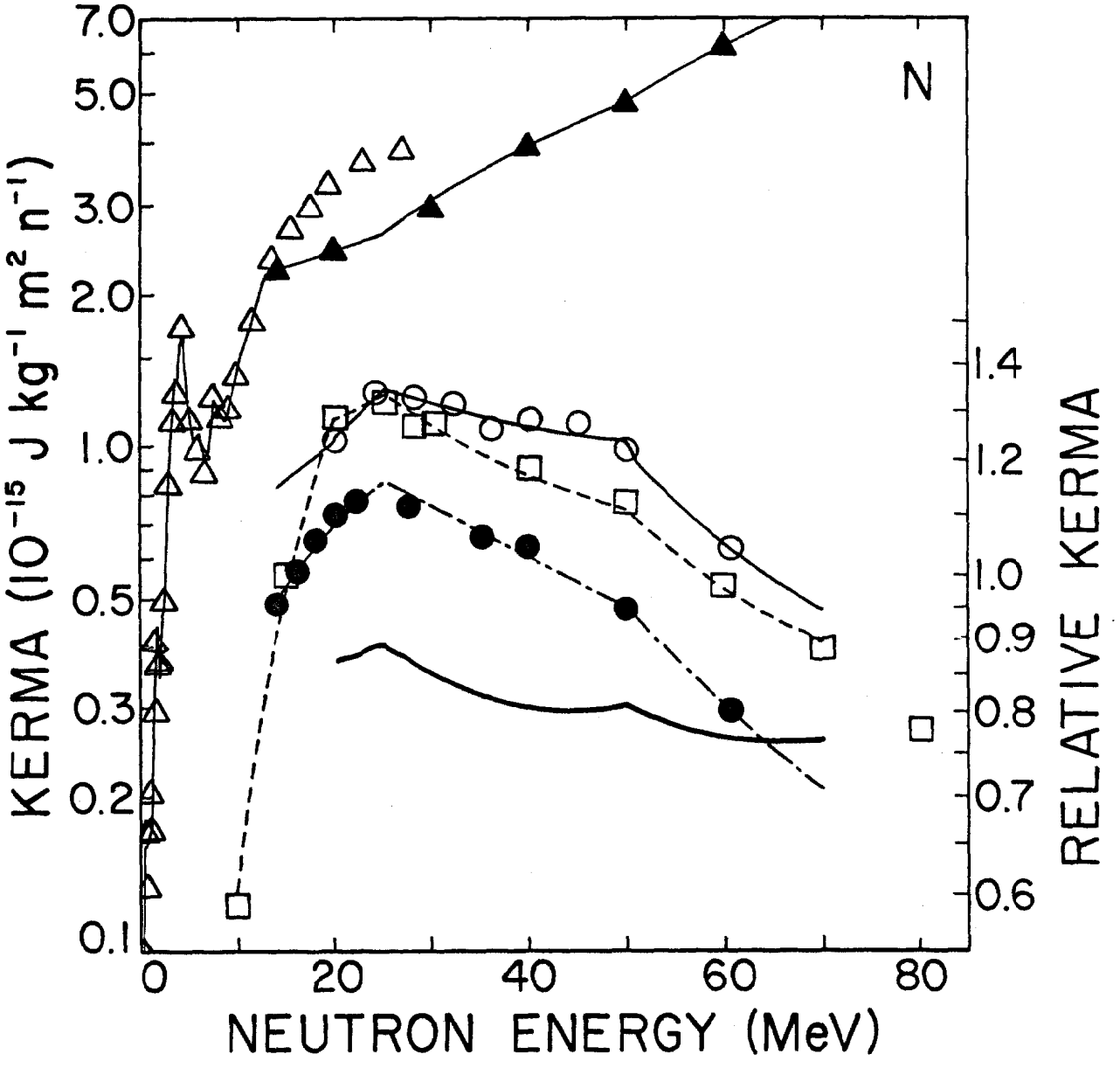
7.0
5.0
3.0
2.0
1.0
0.5
0.3
0.2
0.1
KERMA (10^{-15} J kg^{-1} m^2 n^{-1})
N
1.4
1.2
1.0
0.9
0.8
0.7
0.6
RELATIVE KERMA
0
20
40
60
80
NEUTRON ENERGY (MeV)

Figure 5

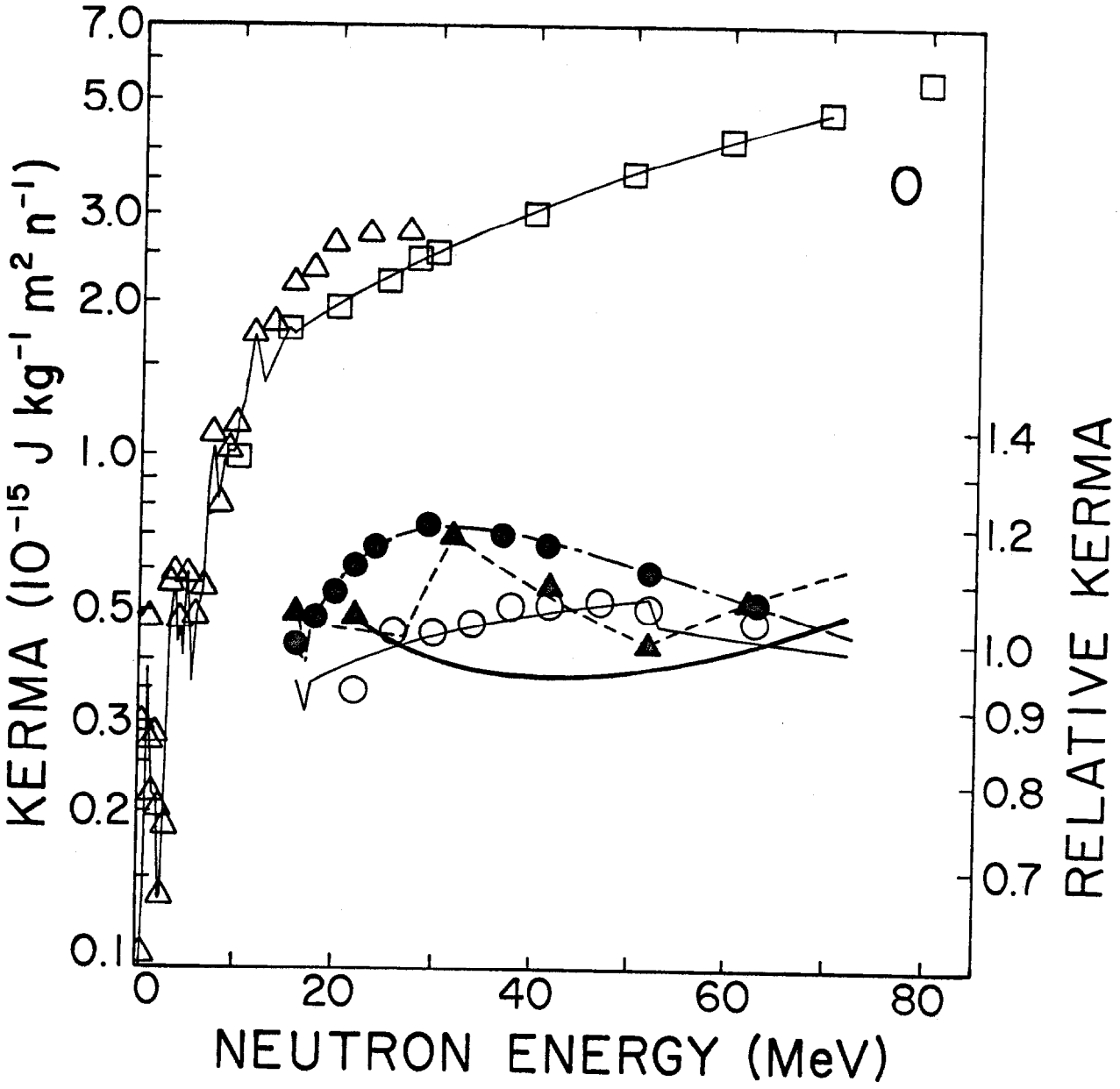
7.0
5.0
3.0
2.0
1.0
0.5
0.3
0.2
0.1
KERMA (10^{-15} J kg^{-1} m^2 n^{-1})
1.4
1.2
1.0
0.9
0.8
0.7
RELATIVE KERMA
0
20
40
60
80
NEUTRON ENERGY (MeV)

Figure 6